JOURNAL OF SOFT COMPUTING AND DATA MINING
e-ISSN: 2716-621X

JSCDM

Vol. 6 No. 1 (2025) 200-229
https://publisher.uthm.edu.my/ojs/index.php/jscdm

Efficient Kidney Cancer Classification from CT Images Using a Lightweight Convolutional Neural Network Optimized with an Enhanced Crow Swarm Optimization Algorithm

Dhuha Abdalredha Kadhim[1], Mazin Abed Mohammed[2]*

[1] *Informatics Institute for Postgraduate Studies, Iraqi Commission for Computer and Informatics, 10011, Baghdad, IRAQ*
[2] *Department of Artificial Intelligence, College of Computer Science and Information Technology, University of Anbar, Anbar, 31001, IRAQ*

*Corresponding Author: mazinalshujeary@uoanbar.edu.iq
DOI: https://doi.org/10.30880/jscdm.2025.06.01.014

Article Info

Received: 13 November 2025
Accepted: 17 May 2025
Available online: 30 June 2025

Keywords

Kidney cancer, CT images, lightweight Convolutional Neural Network, Hybrid Feature Extraction, Crow Swarm Optimization algorithm

Abstract

Kidney cancer is among the fifty most common cancers globally; therefore, early and accurate classification can significantly enhance patient prognosis. However, existing classification models face challenges in effectively handling data obtained from CT imaging. This study proposes a lightweight and automated classification framework for kidney cancer detection using a hybrid feature extraction approach combined with a novel lightweight Convolutional Neural Network (CNN) optimized by a hybrid Crow Swarm Optimization (CSO) algorithm. Two datasets were used for model development and validation: the CT KIDNEY DATASET: Normal-Cyst-Tumor and Stone, containing 12,446 CT images across four classes (normal, cyst, stone, and tumor), and the Kidney Cancer Dataset with 8,400 CT images. For this study, only the normal and tumor classes were used. The feature extraction process employed multiple descriptors to derive relevant features, followed by feature selection optimized using the hybrid CSO algorithm, which demonstrated improved performance. The proposed model achieved 100% accuracy, an F1-score of 97.49%, precision of 97.97%, and recall of 98.28%, with fast processing and successful differentiation of kidney pathologies. This efficient and accurate framework, which integrates deep learning with conventional methods, presents a promising real-time kidney cancer classification system to support radiologists in clinical diagnosis and enhance detection reliability.

1. Introduction

Kidney cancer accounts for 2 to 3% of cancer cases in adults, with men being twice as likely to be affected as women. About 434.840 people develop kidney cancer each year, and about 155.953 die from it, according to World Health Organization estimates for 2022 [1], [2]. Kidney cancer also referred to as renal cell carcinoma (RCC) [3]. Renal tumors are increasing and patients often have the disease for a long time without symptoms, leading to over half of renal cell carcinoma cases being detected by chance. Risk factors for kidney cancer include

smoking, obesity, poor diet, excessive alcohol consumption, hypertension, radiation exposure, and heredity. Radical nephrectomy and partial nephrectomy are considered effective treatments for kidney tumours. Radical nephrectomy removes both the tumour and kidney, while partial nephrectomy only removes the malignant material. The cause of clinic kidney cancer remains unknown [4], [5]. In the past, doctors have mostly used scans like CT, MRI, or ultrasound to find and classify kidney cancer. These methods are used to check kidney lumps' size, shape, and location and see if cancer has spread to other parts of the body. Even though these imaging tools are useful for getting information, many of them can be difficult for people to read and may not always be accurate. Also, telling the difference between non-cancerous and cancerous growths, or figuring out the specific type of kidney cancer, can be hard even for experienced doctors who read scans [6], [7], [8].

Medical imaging has obtained new opportunities through the recent advancements in deep learning technology. CNNs demonstrate superior performance as deep learning models for image classification while beating traditional methods through impressive efficiency together with better accuracy results [9]. These models possess diagnostic automation potential which minimizes human interpretation in diagnostic processes. Deep learning CNN technology uses sizable medical image databases with label markers to determine specific renal cancer characteristics [10]. New images move through these models to receive fast precise measurements about cancer malignancy and cancer type. The utilization of deep learning technology for kidney cancer diagnosis stands at an introductory level [11]. The implementation of deep learning in kidney cancer diagnosis faces several obstacles because of scarce high-quality databases and challenges reading algorithm results and requiring medical professionals to validate outcomes. Deep learning holds great potential for kidney cancer diagnosis and prognosis to benefit patients experiencing this disease [12]. The first step is medical image preprocessing. The second process involved identifying useful features for data classification. This is followed by feature selection, highlighting the best features. The final stage is classification, where images are categorized as normal or abnormal [13]-[17].

The goal of this work is to design a highly accurate but lightweight model for differentiating between kidney cancer and normal tissue based on CT images. The proposed model aims to achieve the best overall accuracy in classification while being computationally efficient to be used in live feeds for clinicians. Our study differs from previous work by incorporating a hybrid model of feature extraction and a lightweight CNN. Further, the study enforces the feature selection process by implementing an optimized Hybrid Crow Swarm Optimization (CSO) algorithm for refining the extracted features leading to better differentiation of normal, cystic, tumor, and stone conditions within kidney images. The intended benefit of this approach is to give radiologists a tool that facilitates accurate identification of kidney cancer and other diseases affecting the kidneys within the shortest time possible. The main contributions of this study are:

- To Develop of multiple feature descriptors that help to select one or more features to be integrated into a new hybrid feature extraction methodology that considerably improves the classification of kidney conditions from CT images.
- To Proposed modified Hybrid Crow Swarm Optimization (CSO) algorithm for feature selection to improve classification based on the best features for the differentiation of kidney pathologies.
- To enhance a lightweight CNN with no significant trade-off between accuracy and computational load that thus can be used in real-world clinical applications.
- Generalization of the proposed model on two large databases of images containing eight thousand four hundred CT scans and describing various changes in the kidneys, including normal, cystic, tumor, and stone.

The rest of the paper is organized as follows. Section 2 presents the related work to detecting CT images. Section 3 describes the methodology, including dataset collection, data preprocessing, and feature extraction. Features selection, and network classifier. Also, Section 4 shows the results and discussion. Lastly, Section 5 presents the conclusion.

2. Related Work

The progress in the field of medical image analysis in the last few years has been based on the concepts of machine learning (ML) and deep learning (DL) that enhance the levels of classification and the rates of accuracy in cancer kinds identification including Kidney cancer. Previously used approaches basically employed hand crafted features with statistical classifiers for detection and diagnoses, but they usually failed to detect complex patterns required for diagnosis in CT images. In the recent past, work has been done using convolutional neural networks (CNNs), and systems that combine the feature extraction and the classification phases into a single framework have been proposed leading to the improved performance of the system. Besides, techniques, such as Particle Swarm Optimization (PSO), and Genetic Algorithms (GA), have been integrated with feature extraction methods for better selection of informative features with higher classification efficiency. However, these models can be very heavy and thus real time application of these models can be a problem. This is because the existing

J. of Soft Computing and Data Mining Vol. 6 No. 1 (2025) p. 200-229

methods do not sufficiently meet the requirements of high accuracy and fast execution when classifying kidney cancer from CT images; therefore, this study extends on these and presents a lightweight CNN and a refined Hybrid crow Swarm Optimization (CSO) algorithm. According to Islam MN. et. al (2022) [18] presented a comprehensive study on the application of Vision Transformers and explainable transfer learning models for the automated detection of kidney cysts, stones, and tumours from CT scan images. It collected and annotated 12,446 images for this purpose, and employed six models, including state-of-the-art Vision Transformer variants (EANet, CCT, and Swin Transformer) alongside traditional models (VGG16, Inception v3, and ResNet50). VGG16 and CCT models performed well, but the Swin transformer was the most effective option for diagnosing kidney stones, cysts, and tumours, achieving an accuracy of 99.30% and demonstrating superior precision, recall, and F1-score. Indicating its potential for enhancing early diagnosis of kidney-related diseases. The limitations of the paper include the lack of comparison with other existing models. Another study by Asif S. et .al (2022) [19] introduced a deep transfer learning (TL) architecture designed to diagnose kidney diseases from CT KIDNEY DATASET: Normal-Cyst-Tumor and Stone' 12,446 CT. The model is built on a pre-trained VGG19 network. It is enhanced by replacing its fully connected layers with a naïve Inception module to improve performance and reduce issues like vanishing gradients and overfitting. The study evaluates two TL strategies: feature extraction and fine-tuning, with the latter achieving a remarkable accuracy of 99.25% in detecting kidney diseases such as cysts, stones, and tumours. The use of Grad-CAM and feature map visualization techniques aids in understanding the model's focus areas in the images, enhancing interpretability. Despite the high accuracy achieved, there were still instances of misclassification. Specifically, two CT images of stones and four CT images of tumors were misclassified.

Also, Narmada et. al (2022) [20] focused on classifying kidney ailments using CT images with a dataset of 12,510 images labeled into 4 classes: cyst, tumor, stone and normal. Utilizing CNN model with Sigmoid and ReLu activation functions. Losing kidney function can be a slow and exhausting process, so the study shows how significant classification is for people's understanding of their state. The proposed model demonstrated good performance in terms of accuracy and precision thus proving that deep learning algorithms can be applied effectively in medical image analysis. achieving almost 99. 36% for evaluation metrics like accuracy, precision & F1 score while for the evaluation time ,99. 38% for recall. However, the limitation of this study is the absence of benchmarking with other models of kidney disease diagnosis or dataset. Dalia Alzu'bi et.al (2022) [21] Proposed to use 2D-CNN methods for the identification of KTs within the computed tomographic images. The researchers specifically analyzed three models: a two-dimensional convolutional neural network with 6 layers also known as the CNN-6, a ResNet50 containing fifty layers and, finally, a VGG16 containing sixteen layers. These models were intended to perform KT (Normal Tumor) detection. The optimal model is 2D (CNN-4) that was proposed for the classification of images as KT as benign or malignant. All the detection models applied in the work including CNN-6, ResNet50, and VGG16 yielded accuracies of 97%, 96%, and 60% respectively. The 2D CNN-4 classification model's accuracy also stood at a 92% at the same time. The study does not include information whether the proposed models were tested on external data set. New study by Abdal basit Mohammed Qadir and Dana Faiq Abd (2023) [22] focused on kidney disease classification to diagnose kidney stones, cysts, and tumors using a dataset of 12,446 CT and whole abdomen images. The study implements a hybrid technique with pre-trained DenseNet-201 for feature extraction and Random Forest for classification, achieving an accuracy rate of 99.44%. The model's performance was evaluated based on accuracy, precision, recall, and F1-score metrics, showcasing significant advancements in AI-based kidney disease diagnosis. The Random Forest classifier, used in the classification stage, is known for its variability, small change in the training data can lead to significant differences in the resulting decision trees. which might affect the consistency of the model's performance. Also, Bhandari et. al (2023) [23] presented a lightweight CNN model with XAI frameworks from CT KIDNEY DATASET: Concerning the Normal-Cyst-Tumor and Stone classification, 12,446 images to diagnose kidney pathologies such as cysts, stones, and tumors with an accuracy of 99,52% that can be supported by interpretive models using LIME and SHAP. The explanations generated by XAI algorithms were considered accurate by the radiologists, indicating the model's potential in acting as a supporting system for IoMT devices. The proposed model achieves higher accuracy than other competitive approaches has fewer parameters and can find target regions in CT images for more accurate diagnosis and treatment of kidney diseases, but the study does not describe whether the proposed models were tested in external datasets or clinical environments.

Faiqa Maqsood et al. (2024) [24] addresses the problem of accurately classifying kidney diseases using CT images. The proposed method, SpinalZFNet, combines SpinalNet and Zeiler Fergus Network (ZFNet) for enhanced feature extraction and classification. This study used a dataset of CT images collected from Dhaka hospitals, including images of normal kidneys, cysts, stones, and tumors. The SpinalZFNet model achieved high performance metrics with an accuracy of 99.8%, sensitivity of 99.9%, specificity of 99.6%, and an F1-score of 99.7%. The study concludes that the SpinalZFNet model offers superior classification performance compared to existing models, making it a viable tool for diagnosing kidney diseases based on CT images. Lucas Aronson et al. (2024) [25] addresses the problem of segmenting kidneys and renal lesions on non-contrast CT images to aid in automated diagnosis. The authors developed a model based on a modified 3D U-Net architecture within the

MIScnn framework, trained on a dataset of 150 non-contrast CT scans split into training and testing sets. The model achieved a high kidney segmentation accuracy with a Dice Similarity Coefficient (DSC) of 0.931 and a lower DSC of 0.711 for renal lesions. Although kidney segmentation was effective, lesion detection faced limitations due to the lack of contrast, which the authors suggest could be mitigated with further training and larger datasets. The study concludes that this deep learning model demonstrates significant potential for clinical use in kidney and lesion segmentation on non-contrast CT images. Table 1 illustrates the summary of the related studies from study goal, dataset used, and limitation.

Table 1 *The summary of the related studies*

Author(s)/Years	Methods/Techniques	Brief Description	Strengths	Weaknesses
Islam et. al (2022) [18]	Swin Transformers	The study developed six models, including Vision transformers and deep learning models, to diagnose kidney diseases, with the Swin transformer outperforming all models in terms of accuracy.	The Swin transformer outperforming all models in terms of accuracy, achieve 99.30% accuracy and providing the best recall	The lack of comparison with other existing models or datasets for kidney disease diagnosis.
Asif et .al (2022) [19]	VGG19 model with naïve Inception	presents a novel deep transfer learning (TL) architecture based on a pre-trained VGG19 model and a naive Inception module for detecting kidney diseases.	This hybrid design helps in extracting robust and discriminative features.	the model is not infallible and may require further refinement to improve its robustness
Narmada et. al (2022) [20]	CNN	using a CNN model with Sigmoid and ReLu activation functions to classify kidney ailments.	The proposed CNN model achieved High ACC 99.36%	The lack of comparison with other existing models or datasets for kidney disease diagnosis
Dalia Alzu'bi et.al (2022) [21]	CNN	models for KT identification: a 6-layered CNN (CNN-6), a 50-layered ResNet50, and a 16-layered VGG16. The final model is a (2D-CNN-4) designed for KT classification.	It has surpassed prior studies in terms of accuracy, with a 97% accuracy rate for tumor detection and a 92% accuracy rate for tumor classification.	The study does not mention whether the proposed models were validated on an external dataset or in a different clinical setting.
Abdalbasit Mohammed Qadir and Dana Faiq Abd (2023) [22]	Random Forest	employs a hybrid technique combining pre-trained DenseNet-201 model for feature extraction and Random Forest for classification.	The hybrid model developed in this study achieved an impressive accuracy.	The Random Forest classifier, used in the classification stage, is known for its variability. A small change in the training data can lead to significant differences in the resulting decision trees.

J. of Soft Computing and Data Mining Vol. 6 No. 1 (2025) p. 200-229

Author(s)/Years	Methods/Techniques	Brief Description	Strengths	Weaknesses
Bhandari et. al (2023) [23]	Customized lightweight CNN	proposes a lightweight CNN model for accurately identifying kidney abnormalities	lightweight CNN model achieved an impressive accuracy of 99.52% for classifying kidney abnormalities	The study does not mention whether the proposed models were validated on an external dataset or in a different clinical setting
Faiq Maqsood et. al (2024) [24]	Spinal ZFNet	This paper presents a novel approach, the SpinalZFNet model, for classification of kidney diseases (normal, cystic, tumorous, and stone) using CT images. The model combines SpinalNet and ZFNet to improve feature extraction and classification performance, supported by preprocessing, segmentation, and feature extraction techniques that help achieve high accuracy, sensitivity, and specificity.	- The SpinalZFNet model achieves outstanding classification performance, outperforming other models in terms of accuracy, sensitivity, specificity, and F1 score. - The approach integrates advanced preprocessing and segmentation techniques (using ENet and feature extraction methods such as WLD-DWT with HOG), improving the reliability of kidney disease detection in CT images.	The model relies heavily on high-quality CT images, and any variation in imaging quality may affect its effectiveness, making generalization across diverse datasets challenging. The computational requirements of SpinalZFNet may hinder real-time applications, especially in resource-constrained environments.

Author(s)/Years	Methods/Techniques	Brief Description	Strengths	Weaknesses
Lucas Aronson et. al (2024) [25]	MIScnn DL framework	The SpinalZFNet model is a hybrid deep learning framework that classifies kidney diseases from CT images into normal, cyst, stone, and tumor categories. It uses advanced pre-processing, segmentation, and feature extraction methods to enhance accuracy and reduce computational costs. The model outperforms existing models in sensitivity, specificity, and F1-score, and incorporates techniques like Weber Local Descriptor and Discrete Wavelet Transform.	The SpinalZFNet model is a highly accurate and efficient tool for kidney disease classification, outperforming traditional models like VGG, DenseAUXNet201, and MLP-ANN. Its enhanced feature extraction capabilities, particularly for kidney disease diagnosis, are facilitated by the combination of SpinalNet and ZFNet. The hybrid SpinalZFNet approach optimizes accuracy and reduces computational overhead, making it suitable for clinical settings with varying computational resources. Overall, the SpinalZFNet model offers promising results in kidney disease diagnosis.	El's performance is influenced by CT image quality, potentially impacting generalizability across medical centers, and its SpinalZFNet architecture requires significant computational resources, potentially limiting its application in resource-constrained settings.

3. Methodology

The methodology for kidney cancer classification from CT images begins with the description of the dataset, In the current work, the used dataset includes a total of the CT Normal – Kidney dataset containing 6,101 CT images and the CT Cyst, Tumor & Stone Kidney – Normal dataset comprising 6,345 CT images together and second is 8,400 CT images from different categories: cyst which originated from normal, tumoral and stone type. The samples are split into the group of healthy samples and the samples which contain some disease to get the best orientation of classification. The method that will be implemented under the proposal of this study involves the following principles. First, preprocessing steps are made to improve image quality and thus decrease the quantity of noise that is essential for the performance of feature extraction. Subsequently, a cross-breeding of feature extraction techniques is conducted to make use of plural descriptors of important characteristics of the images that can be used to discern between renal disorders. Specifically, the extracted features are fine-tuned through a much enhanced Hybrid Crow Swarm Optimization (CSO), for improving feature selection and classification performance. The optimized features are then extracted and passed into a lightweight CNN to categorize the images into the various kidney types. Finally, the model is always checked as well as checking includes factors such as accuracy, precision as well as the recall of the model. Details on each of these steps are provided in the sub-sections below. The details of the proposed kidney cancer classification from CT images using hybrid feature extraction and lightweight CNN enhanced by an improved hybrid CSO algorithm are presented in Figure 1.

J. of Soft Computing and Data Mining Vol. 6 No. 1 (2025) p. 200-229

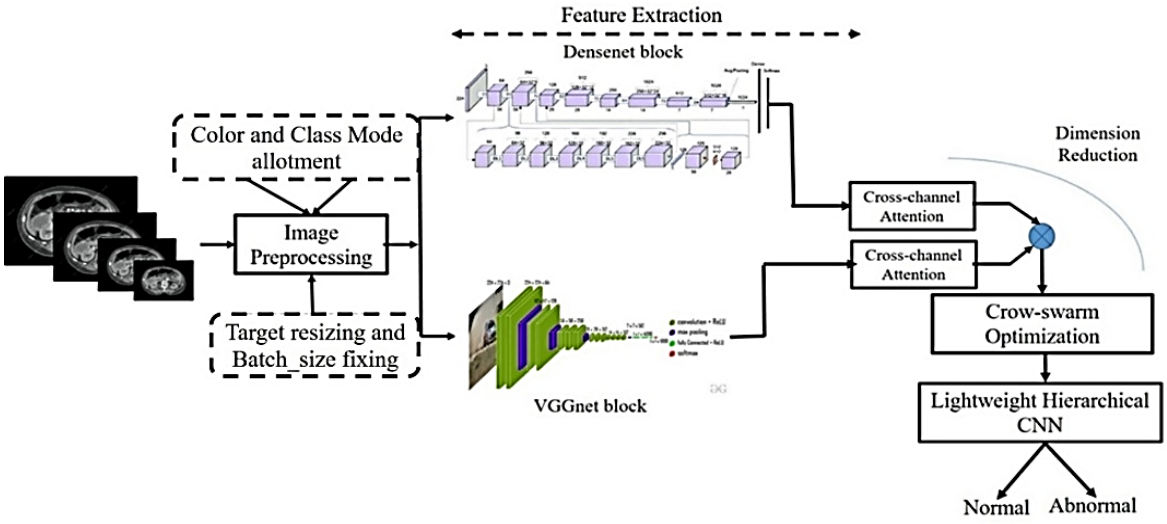

Fig. 1 *The proposed kidney cancer classification from CT images using hybrid feature extraction and lightweight CNN enhanced by an improved hybrid CSO algorithm*

3.1 Datasets Used

In this study, two datasets are used to train and test the proposed kidney cancer classification from CT images using hybrid feature extraction and lightweight CNN enhanced by an improved hybrid CSO algorithm. The details of two datasets are decsribe below:

3.1.1 CT Kidney Dataset: Normal-Cyst-Tumor and Stone

The dataset was collected from PACS at various hospitals in Dhaka, Bangladesh, containing patients diagnosed with kidney tumours, cysts, normal findings, or stones. Coronal and axial cuts were selected from both contrast and non-contrast whole abdomen and urogram studies. Dicom images were created for each radiological finding by selecting diagnoses one at a time. We removed patient information and metadata from the Dicom images and converted them to lossless JPG format. After conversion, a radiologist and medical technologist reverified each image finding for accuracy. Our dataset includes 12,446 unique entries: 3,709 cysts, 5,077 normals, 1,377 stones, and 2,283 tumors.In this study just normal and tumor classes used .Further details are available in [17]. The statistical distribution of all four criteria is given in Table 2.

Table 2 *Distribution of kidney images under different criteria for the CT kidney dataset*

Quantitative measure	No. of scans
Normal	4813
Abnormal	2180
After applying a five-fold cross-validation technique	
Training Set	5595
Testing Set	1398

This dataset is new and requires more exploration by new research studies. A few samples are shown in Figure 2.

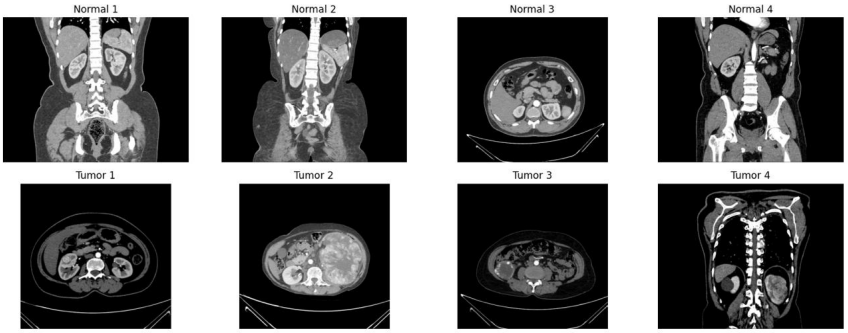

Fig. 2 *Sample images from normal and abnormal classes*

3.1.2 Kidney Cancer Dataset

This dataset consists of 8400 images of 120 adult patients who suspected that they had kidney masses and thus underwent CT scans. However, most of the images are not from the normal (healthy), and abnormal (tumour), therefore ignored in the classification process. Because of this constraint, the number of images in normal and abnormal classes are 2240 and 4200, respectively. The data was obtained from adult patients who were aged between 30 ± 80 years, 55 females and 65 males with CT images of the abdomen and pelvis. The statistical distribution of all four criteria is given in Table 3.

Table 3 *Distribution of kidney images under different criteria for dataset 2*

Quantitative measure	No. of scans
Normal	2240
Abnormal	4200
After applying a five-fold cross-validation technique	
Training Set	5152
Testing Set	1288

Figure 3 shows an example of normal and abnormal SCANS collected from the dataset. Both classes are available in two groups: (1) Train, and (2) Test samples. In the Train set, there are 5152, and in the Test set, the number of images is 1288.

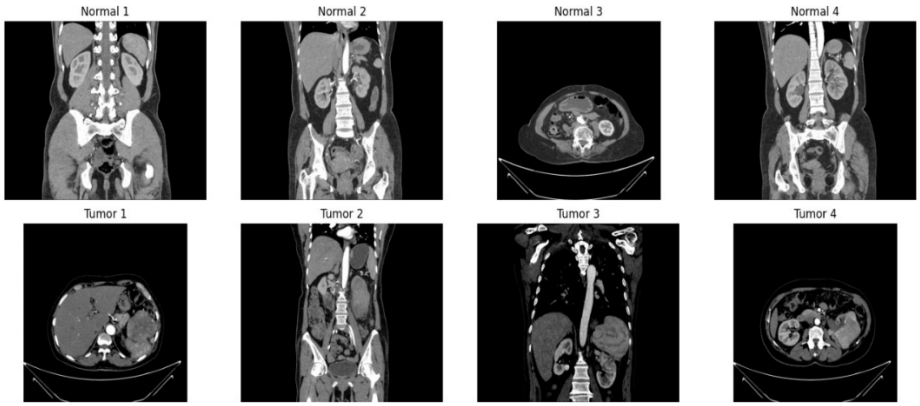

Fig. 3 *Sample images from normal and abnormal classes*

3.2 Preprocessing

Data preprocessing is crucial in medical image processing to standardize the form of images used for disease diagnosis and treatment planning. However, medical images are often noisy, contain artefacts, and have variations in intensity. Challenges include noise, irregularities, and sharpening of edges. To enhance features,

image pre-processing processes like noise elimination, normalization, and enhancement are applied. This work aims to improve data quality.

3.2.1 Data Augmentation

Data augmentation is one of the techniques by which the size of a training dataset can be artificially increased by the introduction of variations of images in a dataset. This entails superimposition, scaling of the elements of the original images as well as translation, rotation as well as flipping of the images, and even color balancing. The reason why data augmentation is used is to enhance the ability of Deep learning models in the generalization of their decisions to enhance the models' robustness and minimize overfitting. In the current case, the following operations are used to generate the new kidney scans and boost the performance of the implementing approach. The augmentation parameters' values such as (rotation 20° and zoom 0.2) were determined through research in previous studies[26]. The details of the applied parameters are given in Table 4.

Table 4 *Details of applied augmentation operations to enhance the performance*

Index	Augmentation Approach	Parameters	Explanation
1	flip	horizontal_flip=True vertical_flip=True	Flip images horizontally/ Vertically
2	rotation	rotation_range=20	Rotate images within the range of -20 to +20 degrees
3	zoom	zoom_range=0.2	Zoom in/out images by up to 20%
4	translation	width_shift_range=0.2 height_shift_range=0.2	Translate images horizontally and vertically by up to 20%
5	contrast	preprocessing_function	Adjust the contrast by a factor of 0.2
6	brightness	preprocessing_function	Adjust the brightness by a factor of 0.2
7	crop	width_shift_range=[-0.2, 0.2] height_shift_range=[-0.2, 0.2]	Crop images by shifting width and height by ±20%
8	height	height_shift_range=0.2	Adjust the height by up to 20%
9	width	width_shift_range=0.2	Adjust width by up to 20%
10	center_crop	preprocessing_function	Center crop to 80% of the image size

3.2.2 Image Normalization

The pixel values of the images are rescaled from their original range of [0, 255] to [0, 1] by multiplying by 1/255. This normalization is useful in enhancing the rate of convergence of the model during training. The training, and testing datasets are rescaled with the help of the ImageDataGenerator class from Keras.

3.2.3 Resizing Image

All the images are then normalized and then resized to a fixed width and height of 60 pixels respectively. This resizing step is important because the majority of the Deep learning models necessitate a set input size.

3.3 Feature Extraction by Hybrid Method

Feature extraction fusion is a strong technique in deep learning in which feature extraction is carried out from various models or data units and which is combined at a further phase. In this method, different sets of features are passed into the network individually by splitting the then recombined or concatenated in a certain number of branches of a neural network before going to the classification/prediction layer. Hence the structure make each branch aim for specific types of features, thus the model will benefit from complementary information derived from each branch to enhance performance. The feature extraction hybridization work shown in Figure 4 integrates DenseNet and VGGNet to produce exceptional results for feature extraction, especially for image classification. The process starts with the preprocessing of the input images, where the image is resized to the target size of 224X224 pixels and the batch size is also standardized across the dataset. Furthermore, the images are defined along the color and class modes in order to optimize the feature extraction step, save essential image data.

Afterwards, characteristics, which are inputs of the decision-making process, are obtained utilizing DenseNet and VGGNet parts. The DenseNet component earns deep and redundant features owing to the connection of layers resulting in the reuse of features without repetition. This structure is beneficial for DenseNet to capture the repeated patterns inside an image hence creating a dense richer representation of the features. At the same time, the VGGNet component is used to extract features from the images due to the network simplicity but with deeper architecture necessary to obtain the texture and other structural properties of the images.

Cross-channel attention mechanisms are applied in an attempt to refine features extracted from both the DenseNet and VGGNet models further. These mechanisms allows the model keep the most important channels of selected feature while filter the other information. This kind of attention process is done two times to enhance the effectiveness of the model's capacity generations for'ya important features and dismissing noisy ones. Cross channel attention mechanism helps in dimensionality reduction by eliminating critical aspects while maintaining such data components for subsequent stages in the process. However, to fine-tune the selected number of the features a crow-swarm optimization method is used that defines which features are more beneficial for the classification task. This optimization approach copies with the ability of crow birds and is used to explore the portfolio of feature space in the hope of arriving at the best feature set. Lastly, the selected features are used as the network input to a low complexity hierarchical CNN that takes the final decision of whether the image is "Normal" or "Abnormal". Such a hierarchical architecture of CNN also helps in classification while keeping the total model's computational complexity relatively low.

The main steps of features extraction using hybrib technique are:

1. Kidney Cancer Images as Input Data:
   The first step is feeding the Kidney Cancer images which are the raw data for classification in this process.
2. The extracted Features using VGG Netmodel:
   - First feature extraction model is VGG Net model.
   - The received kidney cancer images are feed through VGG Net to obtain good features.
   - These extracted features named as VGG Net Features depict some pattern from images. They provide good deep layers that are capable of identifying even the high level features such as edges, texture and shapes that are important for classification.
3. The extracted Features using DenseNet model:
   - For the second, parallel feature extraction model, DenseNet is applied.
   - Some of the images of the kidney cancer are also passed through DenseNet and yields another feature called DenseNet Features.
   - A key aspect for the design of DenseNet is the way the layers of the network are connected, directly to all the previous layers, so the features extracted are richer and more varied. This has advantages of enhancing the general performance of the model in terms of how well it picks on the intricate intricacies and small features on the images.
4. Feature Fusion (Combining VGG Net and DenseNet Features):
   - The features are thereafter fused to obtain the Final Feature Set for VGG Net Features and DenseNet Features.
   - This fusion process involves combining concepts from the VGG Net model particularly in the high level features and DenseNet 121 model in detail information.
   - Integrated feature set offers increased dimensionality of the input images, thus improving the feature space such as decision capability.
5. Output Generation (Final Classification):
   - Final Feature Set is then passed to the classification module which transforms inputs to obtain the Output.
   - The form of this output is a classification result—a decision whether the patient has kidney cancer or not, the severity of the cancer, or its type based on the fused features of both the models.

In kidney cancer classification, late feature fusion can be defined as utilizing deep learning models such as VGG Net and DenseNet to find features of the image according to Equations 1. and 2, respectively. The outcomes of the above-extracted features are then concatenated with each other to get the final feature space. The pseudocode of the late feature fusion process is given in Pseudocode 1.

Pesudocose 1: *late feature hybridization process*

1. Initialize VGG Net and DenseNet models without top layers.
2. Define the input tensor with the shape corresponding to the input images.
3. Pass input tensor through VGG Net to extract features.
  a. Apply a series of convolutional layers with 3x3 filters.
  b. Apply ReLU activation after each convolution.
  c. Apply max-pooling to reduce spatial dimensions.
4. Flatten the output features from VGG Net.
5. Pass input tensor through DenseNet to extract features.
  a. Apply a series of densely connected layers.
  b. Each layer receives input from all previous layers.
6. Flatten the output features from DenseNet.
7. Concatenate flattened features from both networks.
8. Fed into feature reduction step (Crow swarm Optimizer)to reduce the high-dimensionality

Mathematically, the feature map F at a layer l in VGG-net can be represented as

$$F_{i,j}^{k} = \sum_{m,n} W_{mn}^{k} * X_{(i+m).(j+n)} + b^{k} \quad (1)$$

where W_{mn}^{k} are the filter weights, X is the input, and b^{k} is the bias. Similarly, DenseNet explores dense connections where each layer receives inputs from all preceding layers, encouraging feature reuse. The output X_l at layer l is:

$$X_l = H_l\,[X_0,\ X_1,\ X_2, \ldots, X_{l-1}] \quad (2)$$

where H_l is a composite function of batch normalization, ReLU, and convolution operations. The features from VGG Net (V) and DenseNet (D) are extracted separately and then merged according to Equation 3.

$$C = [V, D] \quad (3)$$

Finally, the concatenated features as input to a fully connected layer for the feature reduction step, Figure 4 illustrates the feature extraction fusion process in kidney cancer classification.

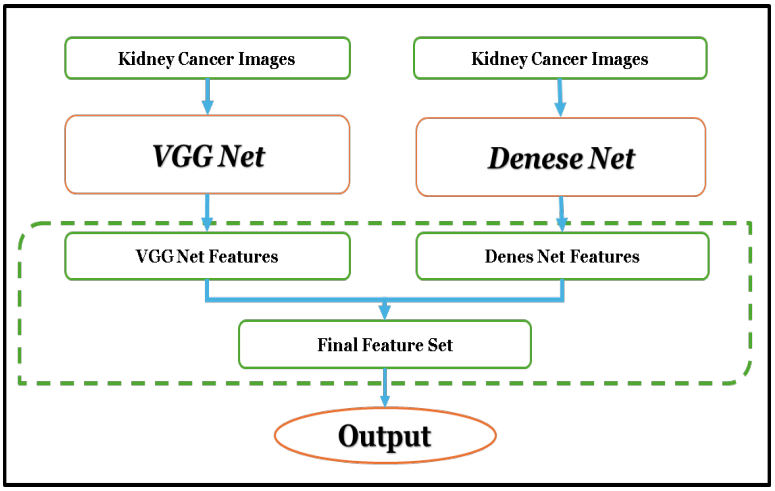

Fig. 4 *Feature extraction fusion process in kidney cancer classification*

3.4 Feature Selection by Improved Hybrid CSO Algorithm

The Improved Hybrid Crow Search Optimization (CSO) algorithm for feature selection searches for the best feature subset and imitates crow behavior with an enhanced Beta hill climbing to refine the local search. The process starts with creating a crow population which for each crow there exists a memory of the best known position. In each step, one crow is picked from the population at random to update the position of another crow, with a probability test being used to decide between the agent utilizing the exploration process on its own or

enhancing its result with the help of the Beta hill climbing process. After each of such updates, the fitness of the new position is computed to check if the it produces a better solution. This process goes back and forth until the algorithm finds a sweet spot in the form of, feature subset which helps in raising the accuracy of the model but is not too greedy to add more features when there can be others that can deliver the same results in one go. The outcome of this procedure can improve feature abstraction and dimensionality reduction by keeping only the most significant features for classification.

Feature reduction in the context of hybrid and the features extracted from cancerous and healthy kidney images using both VGGNet and DenseNet involve the identification of a smaller number of features from a larger feature that contributes towards the intent of our model. The new features are obtained by joining features from VGGNet and DenseNet models whereby features from the previous module are appended to those of the subsequent one. The aim is thus to manage to lower down this feature space while maintaining those aspects that would be helpful in classification applications. To use the hybrid Crow Swarm Optimizer (CSO) with beta hill climbing for feature reduction on hybrid features extracted from kidney images (cancerous and healthy) using VGGNet and DenseNet, follow these steps:

1. **Feature Extraction:** The first step is based on the application of two CNNs, namely VGGNet and DenseNet, with the potential to learn high-level feature vectors from the whole set of kidney images and learn from large image datasets, including ImageNet. Since these kinds of patterns and characteristics are important in differentiating between cancerous tissue and healthy tissues, these models are suitable for building accurate picture descriptions that can be used in the diagnosis of cancer. For each image, a procedure of passing through the pre-trained models of VGGNet and DenseNet to a certain layer would generate two arrays of feature vectors. Then these vectors are concatenated into a single hybrid feature vector for each image. This concatenation makes use of both models, which provides a solidification of the image data.

2. **Hybrid Feature Vector:** Subsequently, from each image, features are extracted from both VGGNet and DenseNet; the feature vectors are then combined. Let v_i stands for the feature vector for the image obtained with the help of feature extraction from VGGNet and d_i refers to the feature vectors extracted from DenseNet for the same image. The hybrid feature vector h_i is then constructed by concatenating these two vectors:

$$h_i = [v_i, d_i] \tag{4}$$

This results in a high-dimensional feature vector that combines the sub-features and feature maps of all the patches detailing them independently by both networks. The feature vector hybridization component now contains additional related information which can be beneficial to increase the effectiveness of classification tasks in the further process. Nevertheless, these dimensions cause high dimensionality in hybrid feature vectors and, therefore, require dimensionality reduction to remove irrelevant or noisy features and improve the learning models' performance.

3. **Fitness Function Estimation:** The fitness function determines the quality of the chosen feature subset. The proposed study uses a fitness function that balances the number of selected features and the classification accuracy:

$$fitness\ (x_i) = w_1 * \left(\frac{reduced\ features}{total\ features}\right) + w_2 * (1 - classification\ accuracy) \tag{5}$$

where reduced features**:** refers to the number of features selected by the optimization algorithm
total features**:** is the total number of features available in the dataset

and w_1 and w_2 are weights that control the trade-off between the number of features and classification accuracy.

4. **Optimization Process:** Each crow's position x_i is a binary vector indicating the selection of features from the hybrid feature vector h_i.

- **Movement Decision**

$$x_i(t+1) = \begin{cases} x_i(t) + r_i * f\left(x_j(t) - x_i(t)\right) & if\ p_{move} > r \\ x_i(t) + \beta * \left(x_{best} - x_i(t)\right) & Otherwise \end{cases} \tag{6}$$

- **Acceptance Probability**

$$p_{move} = \begin{cases} 1 & if\ \Delta f > 0 \\ e^{\frac{\Delta f}{\beta}} & Otherwise \end{cases} \tag{7}$$

Where,

$$\Delta f = f(x_i(t+1)) - f(x_i(t)) \tag{8}$$

J. of Soft Computing and Data Mining Vol. 6 No. 1 (2025) p. 200-229

5. **Algorithm Execution**:
   - Initialize the crow population with random feature subsets.
   - Iteratively update the positions of the crows using the hybrid CSO with beta hill climbing.
   - Evaluate the fitness of each crow's feature subset and update the global best position.
   - Decrease the temperature parameter β according to a cooling schedule.
   - Continue until convergence or a predefined stopping criterion is met.

   The pseudocode for the proposed feature reduction process is given in **Pseudocode 2**.

Pseudocode 2: *Feature Selection algorithm using improved hybrid CSO algorithm*

Initialize the crow population X_i $(i = 1, 2, \ldots, N)$ *with binary vectors representing feature subsets*
Initialize memory for each crow M_i $(i = 1, 2, \ldots, N)$
Set initial temperature β
Repeat *until the stopping criterion is met:*
  For each crow i:
    Select a random crow j (j ≠ i)
    if a random number $r > AP_{ij}$*:*
      Update position using:
      $$x_i(t+1) = x_i(t) + r_i * f\left(M_j(t) - x_i(t)\right)$$
      Compute fitness change:
      $$\Delta f = f(X_i(t+1)) - f(X_i(t))$$
      Compute acceptance probability:
      $$p_{move} = 1 \ if \ \Delta f > 0 \ \ else \ e^{\frac{\Delta f}{\beta}}$$
      if a random number $r < p_{move}$
        Accept the new position $x_i(t+1)$
      else:
        Retain the current position $x_i(t)$
    else:
      Perform beta hill climbing move:
      $$x_i(t+1) = x_i(t) + \beta\,(x_{best} - x_i(t))$$
        Compute fitness change:
        $$\Delta f = f(X_i(t+1)) - f(X_i(t))$$
      Compute acceptance probability:
        $$p_{move} = 1 \ if \ \Delta f > 0 \ \ else \ e^{\frac{\Delta f}{\beta}}$$
        if a random number $r < p_{move}$
        Accept the new position $x_i(t+1)$
      else:
        Retain the current position $x_i(t)$
      Update memory:
      $M_i(t+1) = X(t+1) \ if \ f(X_i(t+1)) < f(M_i(t))$
  Decrease temperature beta according to a cooling schedule
  Update global best position X_{best}
Return the best feature subset found Xbest

The flowchart for the working of the hybrid CSO algorithm is shown in **Figure 5.**

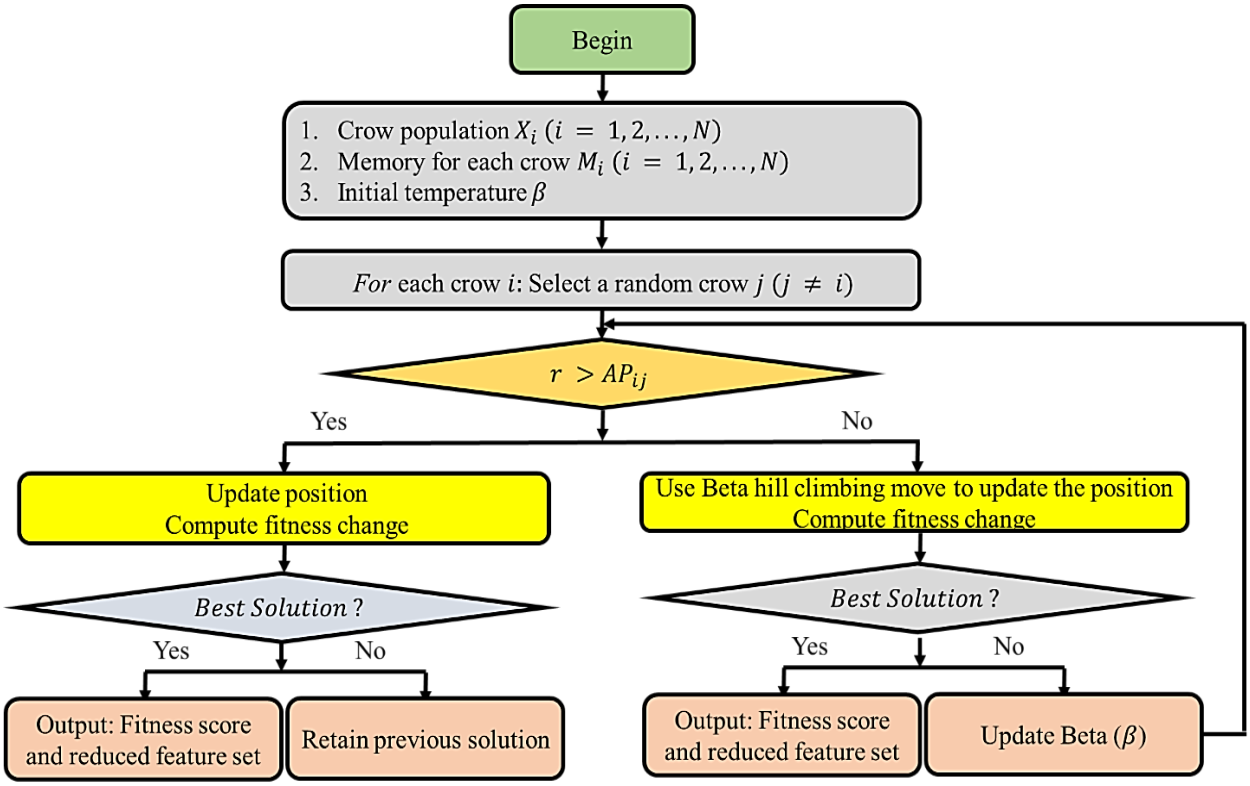

Fig. 5 *Flowchart for proposed hybrid CSO algorithm*

Figure 5, explained Hierarchical representation of data is a model where data is organized into layers, allowing for progressive complexity at each level. This is particularly important in medical imaging, where complex structures require analysis at different levels of granularity. The hierarchical approach is useful for enhancing the identification and diagnosis of specific conditions, such as kidney tumor classification.

In a hierarchical CNN, the layers are pyramid-shaped, with the first few layers detecting simple features like edges and textures, and the subsequent layers fixing complex features like shapes and body parts. This allows CNN to learn and represent different features in a step-by-step manner, enhancing discriminative features and improving classification performance. However, high-dimensional search space remains a challenge in hierarchical data representation in CNN implementation. Heuristic algorithms are known to perform well, especially when dealing with large databases with many variables. They are suitable for a wide range of feature selection problems and can handle different types of data and objective functions.

A new variant of CSO, Hybrid Crow Swarm Optimization (CSO), is used to reduce irrelevant search space and enhance global results. This approach combines two models with excellent feature extraction capabilities of DNNs, focusing on meta-inference optimization towards the feature space. The proposed methodology uses hierarchical but optimal representation capability of data patterns in feature exploration using meta-inference algorithms to improve classification and reduce computational costs.

The hybrid Crow Search Optimization (CSO) algorithm depicted in this diagram combines traditional CSO with a Beta hill-climbing move to improve feature selection and fitness optimization in an iterative process. Initially, the algorithm begins by defining a population of "crows" (representing possible solutions), where each crow XiX_iXi (for i=1,2,...,Ni = 1, 2, ..., Ni=1,2,...,N) has a memory MiM_iMi to store its historical best positions. The algorithm also initializes a parameter β\betaβ, representing the "temperature" that influences the optimization process by controlling exploration and exploitation. This setup phase provides the foundation for the CSO to simulate a natural search behavior with memory retention.

For each iteration, each crow selects another random crow jjj (where j≠ij \neq ij□≠i) to follow and potentially improve its position by mimicking or deviating from the chosen crow's position. At this stage, a random parameter rrr is compared to the awareness probability APijAP_{ij}APij (probability that crow iii is aware of crow jjj's position). If r>APijr > AP_{ij}r>APij, the algorithm updates the crow's position towards the chosen crow and calculates the change in its fitness score. If the crow "discovers" the optimal position by outperforming previous solutions in terms of fitness, it updates its position as the best solution. This memory-based update allows each crow to progressively learn from better solutions within the population.

However, when r≤APijr \leq AP_{ij}r≤APij, the algorithm employs a Beta hill-climbing move—a local optimization technique—to adjust the crow's position incrementally, thus refining the search around the current

solution. This hybrid approach blends the global exploration power of CSO with the local optimization strength of hill climbing, balancing between broad solution exploration and local refinement. After evaluating the best solution achieved, the algorithm either retains the previous solution or updates β\betaβ to modify the search intensity for the next iteration. Ultimately, the process outputs a fitness score and a reduced feature set, yielding a more optimized solution that enhances both the accuracy and efficiency of the model by focusing on key features.

3.5 Hierarchical Lightweight CNN Model

The proposed Hierarchical Lightweight Convolutional Neural Network (CNN) model is a supervised deep learning model optimized for kidney cancer staging by distinguishing between cancerous and normal renal tissues in CT images. This model uses the layer by layer hierarchy, which gradually extracts features of the input images and can characterize both kinds of input information characteristics at the deep and shallow level. Differently from the standard CNN architectures, this design makes it lightweight which decreases the computations' need and the memory demands for the application, thus suitable for near real-time and resource-constrained healthcare scenarios. Such a hierarchy of structures enables the model to zoom in to successively higher levels of detail and promote better localization of different tissue structures important for cancer grading. This organized structure helps to keep only the most significant features given that the improved classification performance achieved has to be efficient.

Kidney cancer staging is the process of identification of cancerous kidney tissues in contrast to normal tissues with the help of medical images containing CT scans or MRIs. To solve this classification problem, a structured and efficient solution is to develop a Hierarchical Lightweight Convolutional Neural Network (CNN) model. The proposed model takes up the hierarchical characteristics of deep learning, and at the same time has the advantage of lightweight and high computational efficiency. The pseudocode 3 Explained the hierarchical lightweight CNN architecture. Firstly, there is a sequence of 3x3 convolutional layers, which is then accompanied by batch normalization and Swish activation to better recognize spatial features in input images. There are max-pooling layers that are employed to down-sample spatial features while retaining important features. Further, residual blocks are used to allow the model to learn deeper features and to solve the vanishing gradient problem to maintain feature maps all through the network. It also improves feature extraction with inception modules that at multiple scales utilise several parallel convolutional layers with different kernel measurements. Dense blocks which are adopted from DenseNet, increase feature reuse and gradient flow while transition layers control the feature map dimensions and network intricacy. The model ended with global average pooling and fully connected layers for the reason that it achieves excellent classification of kidney cancer at last. Parameters were determined through experiments which led to Adam optimizer with a learning rate of 0.001 for 100 epochs yielding optimal results.

Pseudocode 3: *Detailed pseudocode of hierarchical lightweight CNN architecture*

 # Define input shape and number of classes
Input shape: (60, 60, 1)
Number of classes: 2
 # Define the input layer
Inputs <- Input layer with defined shape
 # Convolutional and MaxPooling Block 1
1. Apply Conv2D with 64 filters, kernel size 3x3, stride 1x1, 'same' padding
2. Apply Batch Normalization
3. Apply Swish activation
4. Apply MaxPooling2D with pool size 2x2, stride 2x2
 # Additional Convolutional and MaxPooling Block
5. Apply Conv2D with 96 filters, kernel size 3x3, stride 1x1, 'same' padding
6. Apply Batch Normalization
7. Apply Swish activation
8. Apply MaxPooling2D with pool size 2x2, stride 2x2
9. Apply Global Average Pooling to reduce spatial dimensions
 # Convolutional and MaxPooling Block 3
10. Apply Conv2D with 128 filters, kernel size 3x3, stride 1x1, 'same' padding
11. Apply Batch Normalization

12. Apply Swish activation
13. Apply MaxPooling2D with pool size 2x2, stride 2x2
 # Residual Block 1
14. Pass the output through a Convolutional Block with filter sizes [64, 64, 256], kernel size 3x3, stride 1x1
15. Pass the output through an Identity Block with filter sizes [64, 64, 256], kernel size 3x3
16. Pass the output through another Identity Block with the same configuration
17. Apply MaxPooling2D with pool size 2x2, stride 2x2
18. Apply Global Average Pooling
 # Inception Module 1
19. Apply Conv2D with 128 filters, kernel size 1x1, Swish activation
20. Apply Conv2D with 128 filters, kernel size 1x1, Swish activation
21. Apply Conv2D with 192 filters, kernel size 3x3, 'same' padding, Swish activation
22. Apply Conv2D with 32 filters, kernel size 1x1, Swish activation
23. Apply Conv2D with 96 filters, kernel size 5x5, 'same' padding, Swish activation
24. Apply MaxPooling2D with pool size 3x3, stride 1x1, 'same' padding
25. Apply Conv2D with 64 filters, kernel size 1x1, Swish activation
26. Concatenate all the above outputs to form Inception Block output
 # Residual Block 2
27. Repeat steps 14-18 (Convolutional Block + Identity Blocks + MaxPooling + GAP)
 # Inception Module 2
28. Repeat steps 19-26 (Inception Block)
 # Dense Connection Block
29. Define growth rate as 64 and number of blocks as [6]
30. For each block:
- Pass through a Dense Block with specified growth rate
- If not the last block, apply Transition Block with reduction factor 0.5
31. Apply Batch Normalization
32. Apply Swish activation
33. Apply Global Average Pooling
 # Global Average Pooling Concatenation
34. Concatenate all global average pooling outputs from previous blocks
 # Fully Connected Layer
35. Apply Dropout with rate 0.2 to the concatenated output
36. Apply Dense layer with number of classes as output, using Softmax activation
 # Create and return the model
Return the model with the defined inputs and outputs

3.6 Evaluation

The results of the proposed system were evaluated using the confusion matrix parameters, summarized in Figure 6, which displays the numbers of true positives (TP), true negatives (TN), false positives (FP), and false negatives (FN).

J. of Soft Computing and Data Mining Vol. 6 No. 1 (2025) p. 200-229

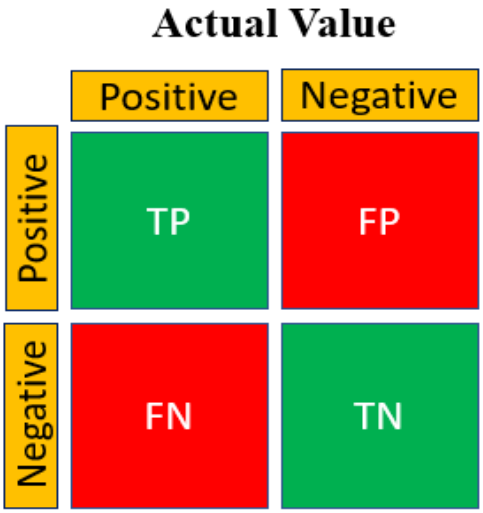

Fig. 6 *The layout of the confusion matrix for the bi-classification problem*

The proposed system was evaluated using four parameters, including the following points:

1. **Accuracy**: is the measure of correctly identified cancerous and non-cancerous cases [27].

$$Accuracy_i = \frac{TP_i + TP_i}{TP_i + TN_i + FP_i + FN_i} \times 100\% \quad (9)$$

2. **Precision** in kidney cancer classification is the ratio of true positive predictions (correctly identified cancer cases) to the total predicted positive cases [28].

$$Precision_i = \frac{TP_i}{TP_i + FP_i} \quad (10)$$

3. **Recall** (**sensitivity**) or true positivity rate, is the percentage of correctly identified cancer cases among all actual positive cases [29].

$$Sensitiviry_i = \frac{TP_i}{TP_i + FN_i} \quad (11)$$

4. The **F1 score** in kidney cancer classification is the harmonic mean of precision and recall, offering a balanced measure of the model's accuracy in identifying cancerous tissues, particularly with uneven class distributions [30].

$$F1\_Score_i = 2 \times \frac{Precision_i \times Sensitivity_i}{Precision_i + Sensitivity_i} \quad (12)$$

4. Results and Discussion

This section outlines the performance of the proposed approach, covering data quality enhancement, feature extraction using VGG and DenseNet models, feature selection with Crow Swarm Optimization (CSO), and a lightweight hierarchical classification method on two datasets. The proposed hybrid features are optimally fine-tuned using CSO, enhancing model efficiency. CSO efficiently explores large search spaces by mimicking the crow's feeding strategy. CSO can efficiently explore the parameter space to identify the optimal configuration of VGG and DenseNet features in hybrid CNNs. Reducing the search space is crucial as it lowers the number of parameters to adjust during training, increasing the training speed. CSO's ability to explore different regions helps avoid local minima, leading to higher optima and faster convergence.

4.1 Preprocessing Results

4.1.1 Data Augmentation for Two Datasets Used Results

1. **First Dataset**: This step is implemented to improve an image dataset1 by creating new copies of the images within it through augmentation and illustrating the improvements made to the given image dataset due to augmentation. Originally, this dataset consisted of Normal/ Healthy (5077 Scans) and Tumor (2283 Scans). The combined dataset is divided into two categories: (1) Training set (5888 scans) and (2) Testing set (1472/1398 scans) using a five-fold cross-validation (80% and 20%)

approach. However, 293 images were highly noisy may cause overfitting during model validation. Therefore, these images are not used during data preprocessing and other steps. However, there is no change in the testing data instance. Further, an augmentation process was implemented to increase the number of images to five times of original training images. The distribution of training instances before and after augmentation is shown in Figure 7.

2.

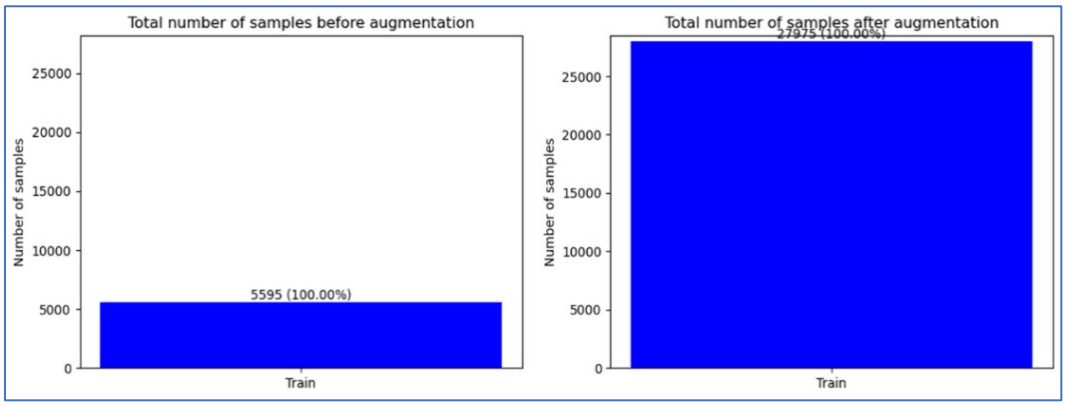

Fig. 7 *The distribution of the training images before and after the augmentation process for the first dataset*

Further, the division of training images as abnormal and normal scans before and after the augmentation process is shown in Figure 8.

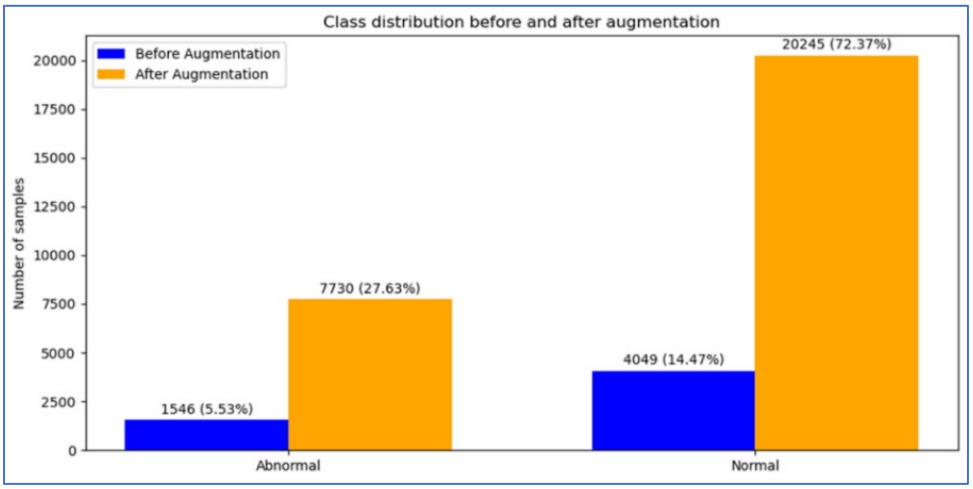

Fig. 8 *The distribution of the training images as abnormal and normal scans before and after the augmentation process for first dataset*

The first row of Figure 9 shows brightness augmentation in which the brightness of the images was modified. The given technique assists in making the model more adaptive to the different input lighting conditions. The second row of images demonstrates the use of contrast changes. Here the authors applied the opposition of the picture's luminosity, which contributes to increasing the difference between the picture's areas. The third row shows instances in which the image has been cropped to draw attention to regions of the image. Cropping allows approximate situations when only a part of an image is significant or images are limited, thus improving the model's ability to pay attention to important detail and not be affected by image size or perspective.

J. of Soft Computing and Data Mining Vol. 6 No. 1 (2025) p. 200-229

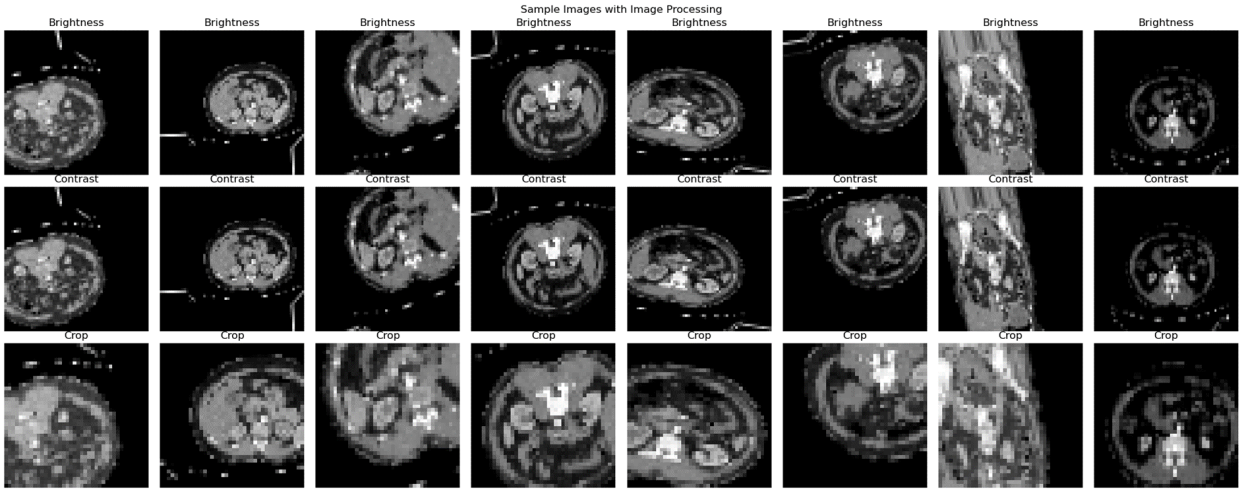

Fig. 9 *Sample images after applying the augmentation procedure using multiple image alteration methods for first dataset*

3. **Second Dataset:** that showed in Figure 10 demonstrates a clear representation of the results obtained from the process of data augmentation on a given data set. The original dataset2 consists of 5,152 samples, according to the histogram. However, after augmenting the data the total counts boosted to 25,760 positions as depicted in the second histogram chart in Figure 9 This gives clear evidence of augmentation's potential in increasing the size of the dataset, an important factor that can considerably enhance the performance of deep learning algorithm.

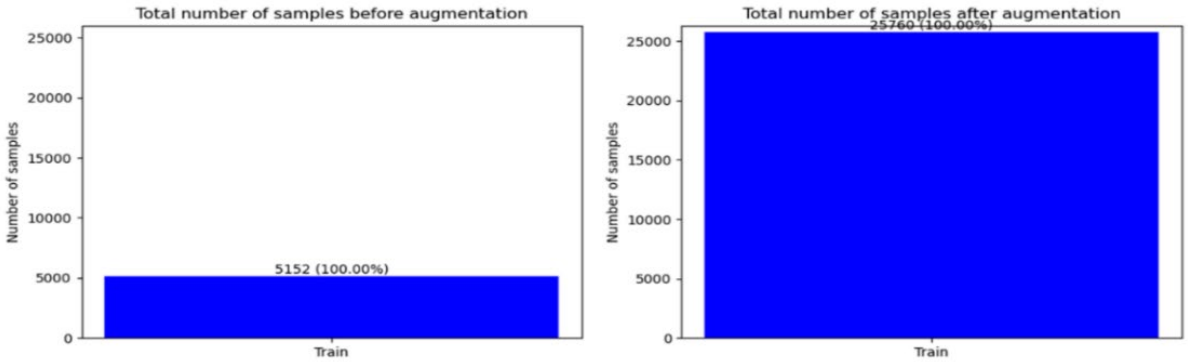

Fig. 10 *Histogram plot of training samples before and after augmentation for second dataset*

Figure 11, the class distribution before and after augmentation is shown for two classes of dataset 2: Positive and Negative for Tumor tissue The interpretation of the final image is as follows: Before augmentation, the "Normal" class had an opportunity to provide 1792 samples while the "Tumor" class had 3360 samples. Speaking of the distribution over the classes, after augmentation, the number of samples in the "Normal" class became 8960, and in the "Tumor" class – 16800. This also illustrates the containment of each class within the overall growth of datasets, and how augmentation contributes to the improvement of balancing the dataset since the number of samples escalates in each class.

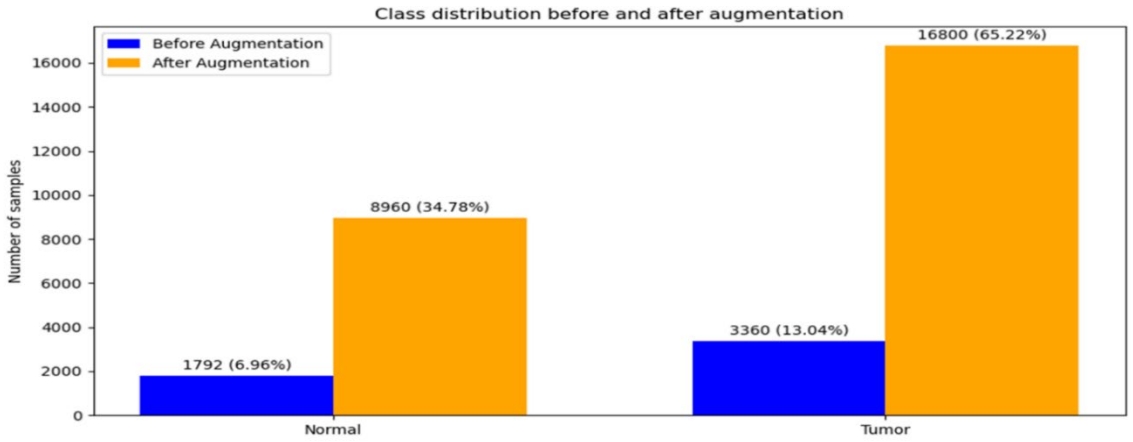

Fig. 11 *Class-wise histogram plot of training samples before and after augmentation for second dataset*

Figure 12 shows the sample images for the kidney cancer classification after applying the image augmentation process. These include the addition of brightness, contrast and addition, cropping, and blanching.

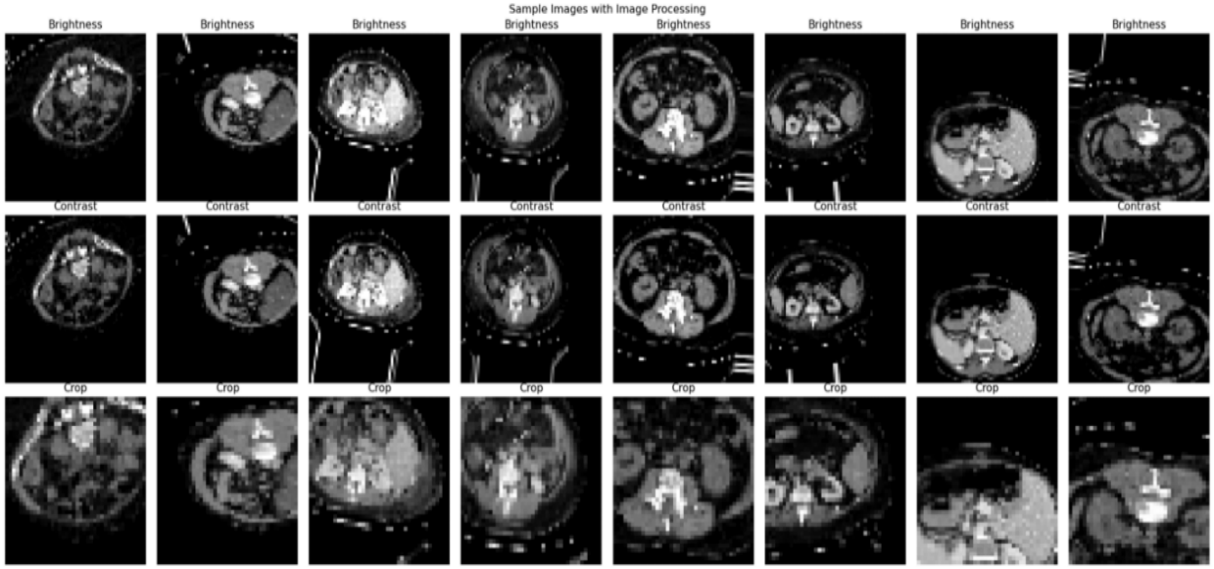

Fig. 12 *Sample images after applying the augmentation procedure using multiple image alteration methods for second dataset*

Although performance enhancement occurred because of augmentation methods which expanded data ranges while minimizing class imbalances and added to model generalizability during the learning phase. The implementation of data augmentation techniques cannot solve all problems that exist in original datasets. While data augmentation strengthens training data it cannot eliminate potential biases which emerge from combination of demographic issues and image artifacts alongside variant acquisition conditions. These subtle issues impact both fairness and real-world viability of the model. Data augmentation serves as an important add-on for training data strength but should be used as an adjunct solution instead of a standalone fix for dataset difficulties.

4.1.2 Data Normalization Results

Data normalization attempt to change range of pixel values from [0, 255] to [0, 1] This normalization is useful in enhancing the rate of convergence of the model during training, and testing.as shown in Figure13.

J. of Soft Computing and Data Mining Vol. 6 No. 1 (2025) p. 200-229

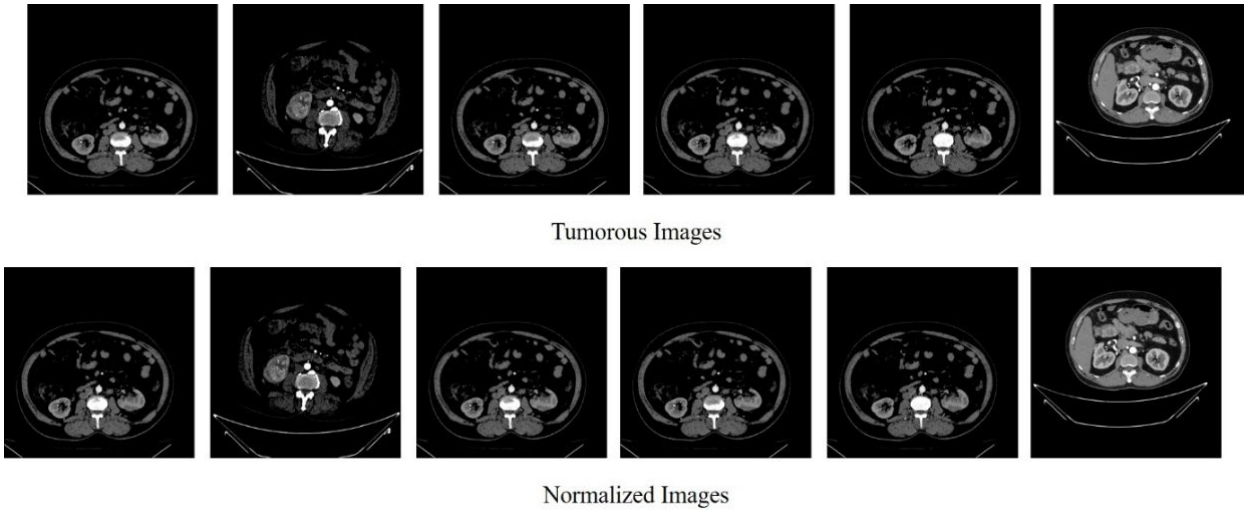

Fig. 13 *Sample images from normal and normalized abnormal classes*

4.2 Feature Extraction Results

For the dataset 1. In the histogram shown in Figure 14, representing column "0", the data shows a roughly normal distribution with a slight skew towards higher values. Here, a total of 1536 features were extracted from Dataset 1 using the proposed hybrid approach. The value of peak frequency is equal to 100 which points to the fact that the most frequently used feature value is of the order of 0. 00025. The values range from slightly above 0.0001 to about 0.00045, with most values of the variable in the region of 0.0002 and 0.00035. This implies that although there is a central tendency of around zero, where everything balances out and equalizes. The values in the cell '00025' present a moderate spread in both directions but shifted slightly to the higher ranks.

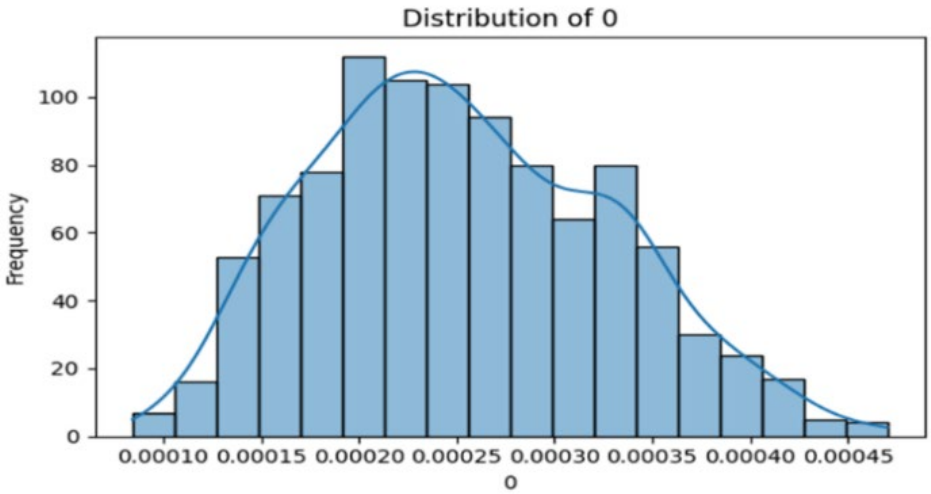

Fig. 14 *Distribution of feature extracted from proposed hybrid in terms of the highest number of non-zero entries for first dataset*

The screenshot of the sample features is shown in **Figure 15**.

A	B	C	D	E	F	G	H
0	1	2	3	4	5	6	7
0	0.000286	0.000349	0	0.000196	6.86E-05	0.000356	6.67E-05
0	0.000154	0.000218	0	5.44E-05	0.000198	0.000147	0.000113
0	0.00032	0.000415	0	0.000181	0.00024	0.000263	8.29E-05
0	0.000239	0.000222	0	0.000125	0.000118	0.000318	7.95E-05
0	0.000112	0.00021	0	7.53E-05	8.25E-05	9.75E-05	9.57E-05
0	0.000348	0.000355	0	0.000193	0.000209	0.000359	0.000121
0	0.000274	0.000452	0	0	0.000212	0.000304	0.000232
0	0.000245	0.000184	0	2.02E-05	8.35E-05	0.000195	7.18E-05
0	0.000514	0.000646	0	0.000187	0.000299	0.00038	0.000235
0	0.000276	0.000428	0	0.000115	0.000158	0.000224	0.000127
0	0.000134	0.000162	0	4.19E-05	6.94E-05	9.85E-05	4.67E-05
0	7.07E-05	9.45E-05	0	7.89E-05	4.09E-05	0.000108	4.14E-07
0	0.000262	0.000257	0	1.69E-05	0.000186	0.00019	0.000138
0	0.000187	0.00029	0	0.000178	7.35E-05	0.000306	0.000124
0	0.000415	0.000548	0	0	0.00023	0.00038	0.000211
0	0.000255	0.000362	0	3.36E-05	0.0002	0.000318	0.000131
0	0.000393	0.000564	0	0.000143	0.000369	0.000294	0.000126
0	0.000118	0.000187	0	3.63E-05	8.36E-05	0.000104	5.85E-05
0	0.000334	0.000323	0	0.000108	0.000393	0.000369	0.000172
0	0.000397	0.000661	0	0	0.000397	0.000569	0.000171
0	0.000389	0.000349	0	0.000125	0.000264	0.000393	0.000125
0	0.000411	0.00039	0	6.75E-05	0.000368	0.000534	0.000228
0	0.000343	0.000448	0	0.000158	0.000268	0.000397	0.000221
0	0.000416	0.000542	0	0.000204	0.000132	0.000405	7.52E-05
0	0.000529	0.000846	0	4.35E-05	0.000414	0.00045	0.000223
0	0.000145	0.000204	0	9.43E-06	0.000135	0.000179	8.81E-05
0	0.000229	0.000366	0	2.74E-05	0.000163	0.000262	6.47E-05
0	0.000182	0.00025	0	0.000117	0.000183	0.000211	6.38E-05

Fig. 15 *Screenshot of the sample features extracted from the proposed hybrid for first dataset*

For the dataset2 the proposed hybrid extracted a total of 1536 spatial feature from the input scans. The histograms (Figure 16) represent the features '513' obtained by the hybrid CNN network of the proposed model. Feature 513 shows a wider distribution, with its values spread from 0.002 to 0.016 and a peak around 0.004. This broader range implies that feature 513 might be responsible for detecting more significant variations or patterns within the data.

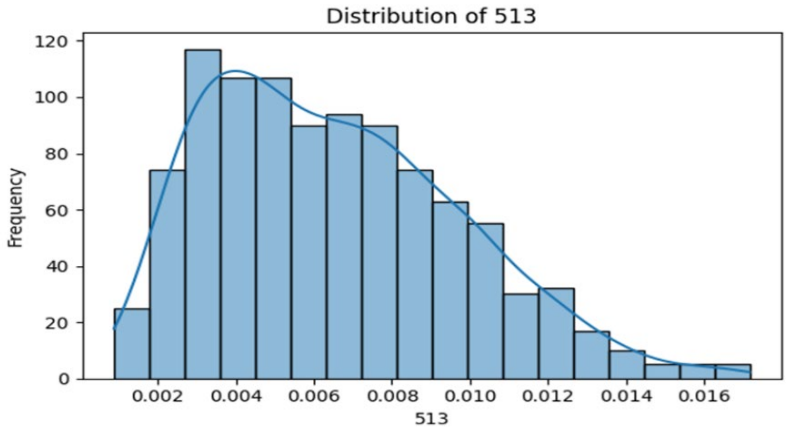

Fig. 16 *Distribution of feature extracted by proposed hybrid based on the highest number of non-zeros entries for second dataset*

J. of Soft Computing and Data Mining Vol. 6 No. 1 (2025) p. 200-229

A sample feature space extracted by proposed hybrid is shown in Figure 17.

0	1	2	3	4	5	6	7
0.000255	9.25E-05	0.000125	0.000192	0.000145	0	8.42E-05	0.000386
0.000215	5.67E-05	8.84E-05	0.000117	0.000168	0	0.000264	0.000478
0.000121	0	5.11E-05	5.04E-05	9.13E-05	0	0.000159	0.000289
0.000177	0	0.000154	0.000187	0.000136	0	0.000342	0.000543
0.000474	0.000153	0.000183	0.000319	0.000294	0	0.000279	0.000851
0.000586	0.000217	0.000319	0.000384	0.000572	0	0.000829	0.001524
0.000344	3.38E-05	0.000227	0.000304	0.000175	0	0.000595	0.000707
0.000176	0	0.000187	0.000151	0.000184	0	0.000237	0.000481
0.000214	0	0.000137	0.000331	0.000191	0	0.000371	0.000689
0.000325	8.56E-07	0.000134	0.000277	0.000225	0	0.000326	0.000673
0.00032	1.49E-05	0.000132	0.000218	0.000257	0	0.000334	0.000629
0.000599	0.000271	0.00036	0.000549	0.000513	0	0.000831	0.001587
0.000481	0	0.000196	0.000425	0.000403	0	0.000655	0.001012
0.000272	5.60E-05	0.00011	0.000242	0.000311	0	0.000327	0.000672
0.000319	2.40E-05	0.000121	0.000242	0.000241	0	0.000493	0.000616
0.000501	0.000524	0.000345	0.000558	0.000557	0	0.000403	0.001134
0.000128	0.000101	9.89E-05	0.000141	0.000143	0	0.000123	0.000341
0.00026	6.80E-05	0.000109	0.000318	0.000215	0	0.000281	0.00068
0.000265	4.43E-05	0.0001	0.000259	0.000187	0	0.000256	0.000548
0.000367	1.27E-08	0.000373	0.000555	0.000464	0	0.000762	0.001316
0.000225	0	0.000195	0.000288	0.000265	0	0.000387	0.000744
0.000307	0.000186	0.000153	0.000307	0.000162	0	0.000332	0.000658
0.000316	3.42E-05	5.61E-05	0.000223	0.000203	0	0.000169	0.000587
0.000283	1.99E-05	0.000228	0.000343	0.000232	0	0.0007	0.00096
0.00081	0.000185	0.000241	0.000472	0.000503	5.65E-05	0.000557	0.001489
0.000219	8.45E-05	0.000135	0.000282	0.000188	0	0.000182	0.00067
0.000651	0.000174	0.000267	0.000392	0.000556	0	0.000771	0.001375

Fig. 17 *Sample feature space extracted by proposed hybrid network second dataset*

4.3 Feature Selection Results

The distributions shown in Figure 18 refer to the results of the CSO algorithm worked out on the features learned by the proposed Hybrid approach, depicting the two features. After the optimization step, the global feature set was reduced to 800 attributes for first Dataset. The first characteristic (marked as '0') tends to be spread out and is not very skewed, with values that appear to be anywhere between -40 to 40. This distribution is a little bit right-shifted, which implies that the targeting of this feature includes a wide range of features. This is basically because the identified feature shows an irregular shape, so it might be capturing high variety patterns of the data in comparison with the others. The second feature (indicated as “528”) is considerably more narrow and it has a mean of zero and a range of about -. 6 to 0. 6. It seems that this value is a less variable characteristic of the feature, as the distribution is very close to the normal distribution, albeit slightly shifted to the left. This indicates that the feature must measure a definite quality of the data that is balanced between samples.

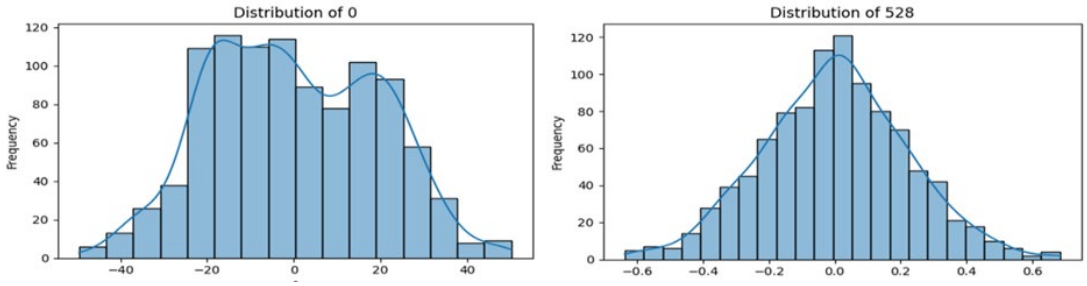

Fig. 18 *Distribution of two features extracted from the proposed hybrid network after applying feature reduction using an improved CSO algorithm for first dataset*

A sample of reduced features is shown in Figure 19.

0	1	2	3	4	5	6	7
0.000197	0.000472	0.000496	0.001133	0.000272	0.00046	0.000108	2.24E-05
0.000352	0.000716	0.00071	0.001262	0.00035	0.000445	0.000179	0
0.000268	0.000759	0.00065	0.001209	0.000331	0.000696	9.59E-05	1.48E-05
0.000155	0.000559	0.000673	0.001254	0.000217	0.000638	0	2.38E-05
0.000317	0.000775	0.000722	0.001218	0.000432	0.000541	0.000144	6.26E-05
0.000267	0.000624	0.000602	0.001121	0.000419	0.00054	0.000177	5.38E-05
0.000203	0.000702	0.000708	0.001079	0.00023	0.000638	9.40E-05	3.93E-05
0.000176	0.000489	0.000451	0.000942	0.000194	0.000499	0.000105	0
0.00015	0.000697	0.000562	0.001171	0.000274	0.000606	0.00015	9.66E-05
0.000154	0.000444	0.000553	0.0011	0.000291	0.000649	0.000176	3.13E-06
0.000231	0.000639	0.000446	0.001165	0.000259	0.000474	0	4.87E-05
0.000414	0.000635	0.000625	0.001269	0.000354	0.000597	6.63E-05	3.89E-05
0.000242	0.000705	0.000654	0.001077	0.00027	0.000644	0.000145	3.98E-05
0.000141	0.00041	0.000417	0.000925	0.000229	0.000431	2.86E-05	8.84E-06
0.000143	0.000674	0.000599	0.001343	0.000333	0.000649	0.000159	0
0.000101	0.000486	0.000471	0.001056	0.000223	0.000427	4.37E-05	2.67E-06
0.000217	0.0006	0.000527	0.001018	0.000159	0.000627	9.95E-05	0
0.000272	0.000822	0.000614	0.001182	0.000278	0.000649	0.000146	3.97E-05
0.000106	0.000502	0.000595	0.001105	0.000274	0.000736	0.000206	3.51E-05
0.000306	0.000666	0.000633	0.0013	0.000302	0.000516	0.000174	3.57E-06
0.000304	0.000807	0.000655	0.001207	0.000372	0.000681	0.000235	2.71E-05
0.000207	0.000771	0.000601	0.001266	0.000297	0.000541	8.32E-05	5.80E-05
0.000164	0.000443	0.000409	0.000963	0.000176	0.000383	4.15E-05	1.47E-05
0.00034	0.00066	0.000568	0.00123	0.000373	0.000754	0.000238	6.45E-05
0.000331	0.000706	0.000722	0.001366	0.000303	0.000633	0.000121	0
0.000297	0.000587	0.000611	0.00133	0.000107	0.000637	0.000189	0
0.000213	0.000604	0.000698	0.001294	0.000275	0.000609	0.000118	0

Fig. 19 *Screenshot of the reduced sample features extracted from the proposed hybrid and an improved CSO algorithm for first dataset*

The application of the CSO algorithm effectively reduced the hybrid feature set to 800 for second datset. Figure 20 presents the frequencies of the most reduced features in the hybrid proposed. Feature 0 deserves an individual analysis as the distribution of its presence in both severities differs also from the rest features. The negative values indicate that the specifically ranked wordings range from about -40 to 80 with the maximum frequency value at about -20. This makes the distribution right-skewed because it has a long tail towards the higher value. This different shape may indicate that this feature is trying to capture a different attribute of the data as compared to the others. The feature 527 which is characterized by distributed frequency that are far more bell-shaped and appear equally likely to be positive or negative, like normal distributions. It could be realized that Feature 527 falls between approximately -0. 4 to 0. 6 but slightly shifted towards the right. These distributions are different meaning that these features are learning-related but different aspects of the input data.

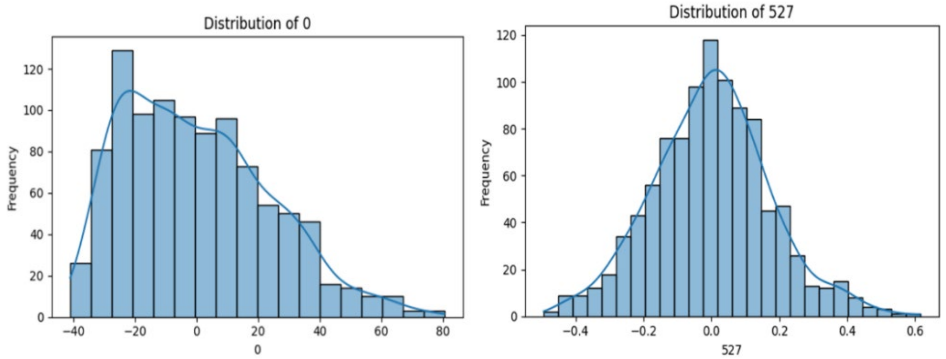

Fig. 20 *Reduced feature distribution of two features extracted by proposed hybrid network based on the highest number of non-zeros entries forsecond dataset*

J. of Soft Computing and Data Mining Vol. 6 No. 1 (2025) p. 200-229

A sample space of the reduced feature space is shown in Figure 21.

0	1	2	3	4	5	6	7
-30.4912	-8.80367	8.019315	1.224674	-0.11484	4.754857	3.396943	2.293083
-17.3437	-10.792	-1.31486	-0.02981	-5.3659	-0.97318	-1.0278	3.633892
-33.8908	-8.02252	-1.91402	-3.87203	-1.99598	-1.37208	-0.13118	-0.06426
-26.6856	3.849646	-3.85221	-1.32079	-0.06064	-2.25022	-1.79735	1.228715
-7.69043	0.318268	7.600567	-2.6524	-7.05709	1.839205	0.015092	-0.71743
58.08435	-11.1153	-1.23089	4.75099	-5.88478	-4.03434	-3.5648	-7.44139
-7.30038	15.16628	-15.9788	0.572342	-3.71385	7.496467	0.759959	-1.30757
-28.8609	7.115705	-3.90395	5.10593	1.876723	-4.28956	-3.58742	0.007078
-14.0998	-0.43964	-2.58432	-7.40887	1.24629	-2.11025	0.275445	-2.26386
-6.73096	-5.15071	-4.00166	-7.772	2.600612	-1.83272	1.801946	-4.12448
-11.4477	-4.45074	-3.00692	-5.96878	-0.00377	-1.18767	-0.19348	3.902917
62.66759	-13.58	-12.0483	9.094113	-8.04304	-2.11737	3.437076	-3.44418
17.05802	7.71071	-12.787	-10.8652	4.96347	1.499246	2.6314	5.307317
-2.71604	-10.8034	-0.57032	-2.87243	4.455316	0.032837	-0.38381	1.933786
-1.31049	-2.86812	-13.3985	-6.05855	1.507799	-0.00888	5.474014	-2.37415
19.66532	-14.0179	16.81735	12.20713	7.103739	14.8505	-4.54546	10.64752
-26.9303	-15.7247	4.119194	2.475505	1.841953	2.285983	-1.20231	-0.98347
-19.1924	-3.51175	4.228545	-5.04914	0.958807	-0.42308	0.005383	-2.01956
-22.6468	-4.62684	1.918824	-5.5464	0.919766	-0.53473	-0.7269	-0.98678
2.909785	36.3681	-6.2792	9.8196	8.199032	-9.52981	-6.31976	2.431219
-20.3609	11.35919	-2.71729	1.833406	2.498901	-3.07844	-2.10859	2.333703
-3.24045	-12.3174	-2.72709	3.162482	-5.50969	-1.04144	-0.45375	7.134009
-20.6161	-5.42358	6.159131	-1.59793	-4.31548	-1.21467	-1.29666	-2.12955
-7.85967	22.72496	-11.9515	6.219541	-0.36109	2.194815	-4.867	0.972116
29.4441	2.226221	10.59672	1.670171	-10.4628	-1.70858	-5.41061	-5.77188
-17.5784	-8.34026	5.610699	0.474352	-2.71325	-1.62005	-2.68227	-3.48608
38.85456	-3.35162	-8.61465	0.706576	-11.7427	-0.33428	0.360433	3.791872

Fig. 21 *Sample reduced feature space extracted by proposed hybrid for second dataset*

In figure 22 illustrates how Crow Swarm Optimization (CSO) improved the performance metrics of the model through its application in feature selection process. The model transition from 1536 to 800 features produced enhanced metrics that included better accuracy, precision, Recall and F1 score performance.

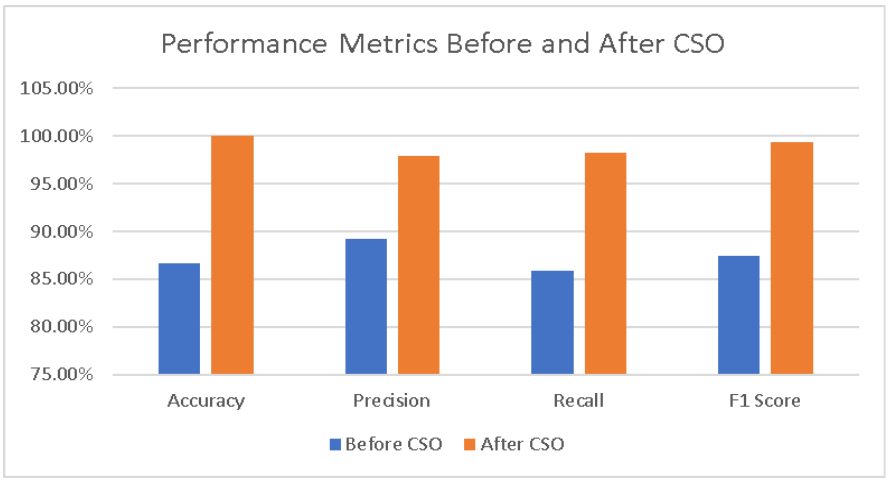

Fig. 222 *Performance metrics before and after CSO*

4.4 Classification Results

The proposed method has a higher possibility of generating good results. It scored the best possibility accuracy of 100% and nearly the best ROC AUC of 0.99. The following confusion matrix demonstrates that the misclassification errors in the image data are minimal, which is evident with values of precision equal to 0.9797, recall of 0.9828, and F-score of 0.9794. This model shows high performance, which is probably explained by the success achieved in the inclusion of simple features and classification capabilities, which is indicated by the low loss value. The confusion matrix and ROC curve of the proposed method are given in Figure 23.

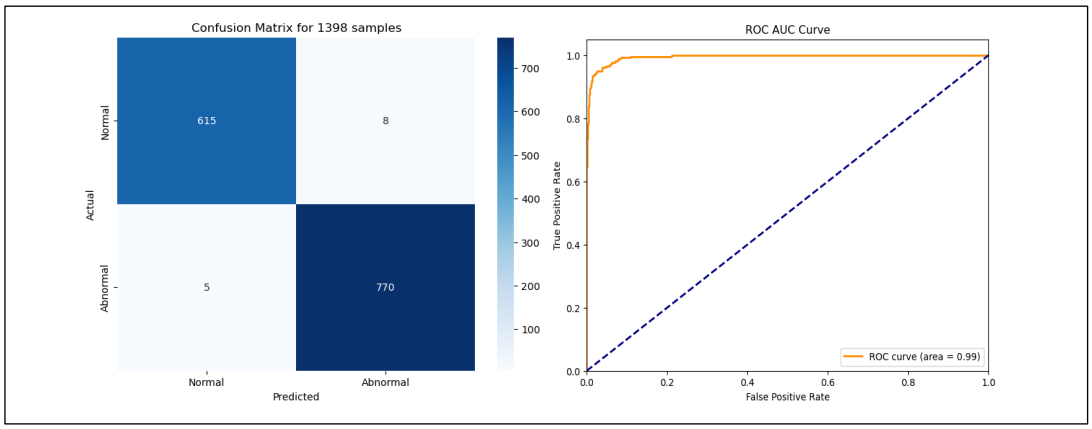

Fig. 23 *The area under the curve (right) and confusion matrix (left) was realized using the proposed hybrid model for first dataset*

Each model's results are presented with a confusion matrix and a Receiver Operating Characteristic (ROC) curve on second dataset. the confusion matrix with ROC curve for the proposed hybrid network are illustrated in Figures 24 the proposed hybrid CNN model demonstrates outstanding performance, achieving near-perfect classification results. It correctly classified 668 normal and 600 abnormal cases, with minimal misclassifications-only 11 normal and 9 abnormal cases were incorrectly labeled. The ROC curve's AUC of 1.00 signifies perfect discriminative ability. The proposed method's accuracy of 99.26% and exceptionally high precision, recall, and F-score values underscore its superior effectiveness for kidney cancer classification.

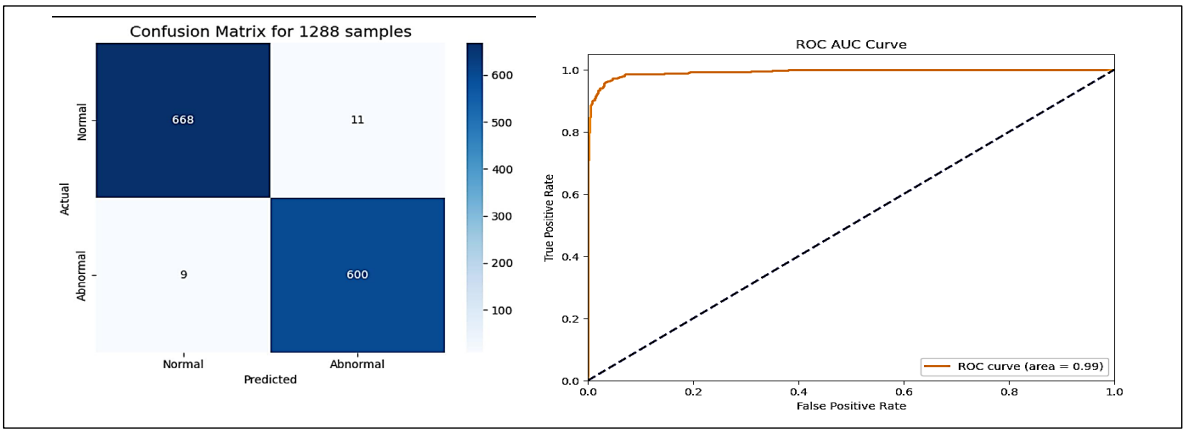

Fig. 24 *The area under the curve (right) and confusion matrix (left) realized in the proposed hybrid CNN classification using an improved CSO algorithm for feature reduction for the second Dataset*

J. of Soft Computing and Data Mining Vol. 6 No. 1 (2025) p. 200-229

Table 5 presents a comparative analysis between the proposed study and existing approaches from the literature, highlighting key differences in methodology, performance, and innovation

Table 5 *Comparison table between the proposed system and the literature review papers*

Author / Year, Ref	Method Used	Accuracy	F1-score	Precision	Recall
Islam et. al (2022) [18]	Swin Transformers	99.30%	99.6%	99.3%	99.4%
Asif et .al (2022) [19]	VGG19 model with naïve Inception	99.25%	N/A	N/A	N/A
Narmada et. al (2022) [20]	CNN	100%	N/A	100%	100%
Dalia Alzu'bi et.al (2022) [21]	CNN	97%	97%	96.5%	96.5%
Abdalbasit Mohammed Qadir and Dana Faiq Abd (2023) [22]	Random Forest	99.44%	99.425%	99.45%	99.475%
Bhandari et. al (2023) [23]	Customized lightweight CNN	99.52%	99.7%	99.475%	99.75%
Faiq Maqsood et. al (2024) [24]	Spinal ZFNet	99.8%	99.7%	99.6%	99.9%
Lucas Aronson et. al (2024) [25]	MIScnn DL framework	69%	77%	77%	77%
Our Proposed	CNN-lightweight with CSO	100%	99.32%	97.97%	98.28%

This table compares different deep learning and machine learning models based on their performance measures: Accuracy, F1-score, Precision, and Recall. The table shows methods from studies done between 2022 and 2024. It allows for an easy comparison with the new system in 2024, which uses a lightweight CNN design along with Crow-Swarm Optimization (CSO). The "Swin Transformers" model from 2022 shows great results with an accuracy of 99. 30% It also has F1-score, precision, and recall all close to 99%, which means it works very well in finding the right answers without missing too many. Another model from 2022 that uses the "VGG19 model with simple Inception" also gets a high accuracy of 99. 25% However, it doesn't provide information on F1-score, precision, and recall, so it's hard to judge how well it balances precision and recall. CNN models from 2022 have different levels of performance. One model reached perfect scores, achieving 100% accuracy, precision, and recall. Another model did not do as well, getting 97% accuracy and 96. 5% for precision and recall. This shows that the effectiveness of CNN models can vary depending on how they are set up or the data they use. In 2023, a Random Forest model achieved great results with an accuracy of 99. 44% Its F1-score, precision, and recall were all around 99. 4%, showing that it works well for classification tasks, even though it's an older type of machine learning method. Also, a "Customized lightweight CNN" from 2023 was able to reach 99. 52% Its precision and recall are about 99. 75%, which means it did a good job of finding the important details without using too much computing power. Later in 2024, Spinal ZFNet performs very well, reaching 99. 8% accuracy and balanced precision and recall scores of 99. 7% and 999% At the same time, the "MIScnn DL framework" has a much lower accuracy of 69%. Its F1 score, precision, and recall are all at 77%, showing that it is not very effective for this task. The proposed method, CNN-lightweight with CSO, works better than other methods and has a perfect score of 100%. It also has a high F1-score of 99. 32%, precision of 97. 97%, and recall of 98. 28% This shows that it performs well and is balanced in all areas. Adding Crow-Swarm Optimization helps improve accuracy while keeping precision and recall high. This means it suggests the best way to choose features and train the model effectively. This comparison shows that the suggested system is a great choice for classifying things, as it is both accurate and works quickly.However, The strong classification achievement demonstrated by the hierarchical lightweight CNN classifier faces an essential limitation because it does not provide explanations about its behavior. The model operates as a black box because its complex architecture makes it difficult to understand which features contribute to its decisions. The lack of explainability may present issues in clinical work since both transparency and trust play crucial roles. The model exhibits dependable performance through metrics but its hidden reasoning process remains unclear to the users.In addition in this limitation, The model's generalization abilities represent another major issue that needs attention. The proposed hierarchical lightweight CNN classifier demonstrated outstanding results on the collected datasets yet lacks proof of how it performs on unknown external data. Training and validation run using particular datasets excluded the complete range of demographic and scanner variations and protocol differences taken in actual clinical practice. Performing well on specific datasets does not guarantee reliable performance once the model extends its use to varied and heterogeneous patient populations. Additional testing of the model through independent datasets becomes necessary to confirm its performance stability in various clinical conditions.

5. Conclusions

This study presents a comprehensive and efficient approach to kidney cancer classification from CT images using a hybrid methodology that combines deep learning with a novel feature selection process. The proposed system leverages a lightweight Convolutional Neural Network (CNN) enhanced by a hybrid Crow Swarm Optimization (CSO) algorithm, specifically optimized for high accuracy and low computational load. This model's architecture is designed to achieve a robust balance between feature richness and computational efficiency, ensuring it can handle real-time clinical applications effectively. By integrating hybrid feature extraction from VGGNet and DenseNet with an optimized CSO algorithm, the framework enhances both the discriminative power and processing speed, making it suitable for practical deployment in healthcare environments. The experimental results demonstrate the effectiveness of this model, achieving high metrics across accuracy, F1-score, precision, and recall. Notably, The hybrid CNN-CSO model achieved a 100% accuracy score because of its implementation with cross-validation techniques. The evaluation across various data subsets through this approach minimized overfitting and confirmed that results would apply to new data samples, reflecting its capability to reliably differentiate between normal and abnormal kidney tissues. The feature selection process, guided by the CSO algorithm, was critical in reducing dimensionality without compromising performance, allowing the model to focus on the most relevant features extracted from the CT images. This methodology not only improves diagnostic accuracy but also provides a faster processing time, thus supporting the rapid assessment necessary in clinical settings. Despite its promising results, the study acknowledges limitations related to dataset variability and generalizability. Research should focus on several directions to increase the clinical usefulness and adaptability of the proposed CNN-CSO hybrid model. The training and validation of the model used specialized datasets that affect its broader use across diverse patient demographics and different imaging environments but additional datasets could enhance widespread acceptance. External testing of the model using independent data should be implemented to establish its reliability across different clinical applications. The real-time implementation of this system would help integrate it smoothly into clinical workflows to enable quick decision-making processes. The incorporation of Grad-CAM as an explainable AI technique would enable visual presentation of key CT image sections that primarily affected the model's decision process thus increasing doctor confidence in system operations. A federated learning system represents a way to train collaborative models between institutions while protecting their data thus resulting in better diagnostic applications for widespread use. Overall, the proposed hybrid CNN-CSO model contributes significantly to advancing automated kidney cancer diagnosis, offering a valuable tool for radiologists in early detection and treatment planning.

Acknowledgement

The authors acknowledge the support from Iraqi Commission for Computer and Informatics and University of Anbar throughout this project.

Conflict of Interest

The authors declare no conflict of interests regarding the publication of the paper.

Author Contribution

The authors' contributions to this work are as follows: ***Designed and conceptualized the study:*** *Dhuha Abdalredha Kadhim and Mazin Abed Mohammed;* ***data collection:*** *Mazin Abed Mohammed;* ***analyzed and explained the results:*** *Dhuha Abdalredha Kadhim and Mazin Abed Mohammed;* ***write drafted and final versions of the manuscript:*** *Dhuha Abdalredha Kadhim and Mazin Abed Mohammed. After reviewing the results, all authors approved the final draft of the manuscript.*

References

[1] International Agency for Research on Cancer (IARC). (2022). Cancer fact sheet: World. Global Cancer Observatory. Retrieved from https://gco.iarc.who.int/media/globocan/factsheets/populations/900-world-fact-sheet.pdf

[2] Abdalredha Kadhim, D., & Abed Mohammed, M. (2024). A Comprehensive Review of Artificial Intelligence Approaches in Kidney Cancer Medical Images Diagnosis, Datasets, Challenges and Issues and Future Directions. International Journal of Mathematics, Statistics, and Computer Science, 2, 199–243. https://doi.org/10.59543/ijmscs.v2i.9747

[3] Abdalredha Kadhim, D., & Abed Mohammed, M. (2025). Advanced Machine Learning Models for Accurate Kidney Cancer Classification Using CT Images. Mesopotamian Journal of Big Data, 2025, 1-25. https://doi.org/10.58496/MJBD/2025/001

[4] Mohammed, M. A., Lakhan, A., Abdulkareem, K. H., Deveci, M., Dutta, A. K., Memon, S., ... & Martinek, R. (2024). Federated-Reinforcement Learning-Assisted IoT Consumers System for Kidney Disease Images," in *IEEE Transactions on Consumer Electronics*, 70, 4, 7163-7173. https://doi: 10.1109/TCE.2024.3384455

[5] Moon, H. S. (2014). Biological effects of conjugated linoleic acid on obesity-related cancers. Chemico-Biological Interactions, 11, 006. https://doi.org/10.1016/j.cbi.2014.11.006

[6] Chen, G., et al. (2020). Prediction of chronic kidney disease using adaptive hybridized deep convolutional neural network on the internet of medical things platform. IEEE Access, 8, 2995310. https://doi.org/10.1109/ACCESS.2020.2995310

[7] Shon, H. S., Batbaatar, E., Kim, K. O., Cha, E. J., & Kim, K. A. (2020). Classification of kidney cancer data using cost-sensitive hybrid deep learning approach. Symmetry (Basel), 12(1), 10154. https://doi.org/10.3390/sym12010154

[8] Vijayarani, S., Sivamathi, C., & Tamilarasi, P. (2023). A hybrid classification algorithm for abdomen disease prediction. ASEAN Journal of Science and Engineering, 3(3), 45677. https://doi.org/10.17509/ajse.v3i3.45677

[9] Abdelrahman, A., & Viriri, S. (2022). Kidney tumor semantic segmentation using deep learning: A survey of state-of-the-art. Journal of Imaging, 8(3), 55. https://doi.org/10.3390/jimaging8030055

[10] Tahir, F. S., & Abdulrahman, A. A. (2023). Kidney stones detection based on deep learning and discrete wavelet transform. Indonesian Journal of Electrical Engineering and Computer Science, 31(3), 1829-1838. https://doi.org/10.11591/ijeecs.v31.i3.pp1829-1838

[11] Almarzouki, H. Z. (2022). Deep-learning-based cancer profiles classification using gene expression data profile. Journal of Healthcare Engineering, 4715998. https://doi.org/10.1155/2022/4715998

[12] Wasi, S., Alam, S. B., Rahman, R., Amin, M. A., & Kobashi, S. (2023). Kidney tumor recognition from abdominal CT images using transfer learning. In Proceedings of The International Symposium on Multiple-Valued Logic (pp. 21). https://doi.org/10.1109/ISMVL57333.2023.00021

[13] Gupta, S., Gupta, M. K., Shabaz, M., & Sharma, A. (2022). Deep learning techniques for cancer classification using microarray gene expression data. Frontiers in Physiology, 952709. https://doi.org/10.3389/fphys.2022.952709

[14] Jackson, P., Hardcastle, N., Dawe, N., Kron, T., Hofman, M. S., & Hicks, R. J. (2018). Deep learning renal segmentation for fully automated radiation dose estimation in unsealed source therapy. Frontiers in Oncology, 8, 215. https://doi.org/10.3389/fonc.2018.00215

[15] Prakash, A. M., Aditya, S., Diwakar, S., Santosh, P., & Hema, N. (2023). Tumor detection using deep learning in organs specific to Indian predicament. In Proceedings of CONECCT 2023 - 9th International Conference on Electronics, Computing and Communication Technologies (10234765). https://doi.org/10.1109/CONECCT57959.2023.10234765

[16] Abdelrahman, A., & Viriri, S. (2023). EfficientNet family U-Net models for deep learning semantic segmentation of kidney tumors on CT images. Frontiers in Computer Science, 5, 1235622. https://doi.org/10.3389/fcomp.2023.1235622

[17] Lubbad, M., Karaboga, D., Basturk, A., Akay, B., Nalbantoglu, U., & Pacal, I. (2024). Machine learning applications in detection and diagnosis of urology cancers: A systematic literature review. Neural Computing and Applications. https://doi.org/10.1007/s00521-023-09375-2

[18] Islam, M. N., Hasan, M., Hossain, M. K., Alam, M. G. R., Uddin, M. Z., & Soylu, A. (2022). Vision transformer and explainable transfer learning models for auto detection of kidney cyst, stone and tumor from CT-radiography. Scientific reports, 12(1), 11440. https://doi.org/10.1038/s41598-022-15634-4

[19] Asif, S., Wenhui, Y., Jinhai, S., Ain, Q. U., Yueyang, Y., & Jin, H. (2022). Modeling a fine-tuned deep convolutional neural network for diagnosis of kidney diseases from CT images. In Proceedings of the 2022 IEEE International Conference on Bioinformatics and Biomedicine (BIBM), 5615. https://doi.org/10.1109/BIBM55620.2022.9995615

[20] Narmada, N., Shekhar, V., & Singh, T. (2022). Classification of kidney ailments using CNN in CT images. In 2022 13th International Conference on Computing Communication and Networking Technologies (ICCCNT), 4256. https://doi.org/10.1109/ICCCNT54827.2022.9984256

[21] Alzu'Bi, D., et al. (2022). Kidney tumor detection and classification based on deep learning approaches: A new dataset in CT scans. Journal of Healthcare Engineering, 3861161. https://doi.org/10.1155/2022/3861161

[22] Qadir, A. M., & Abd, D. F. (2023). Kidney diseases classification using hybrid transfer-learning DenseNet201-based and random forest classifier. Kurdistan Journal of Applied Research, 11. https://doi.org/10.24017/science.2022.2.11

[23] Bhandari, M., Yogarajah, P., Kavitha, M. S., & Condell, J. (2023). Exploring the capabilities of a lightweight CNN model in accurately identifying renal abnormalities: Cysts, stones, and tumors, using LIME and SHAP. Applied Sciences, 13(5), 53125. https://doi.org/10.3390/app13053125

[24] Maqsood, F., et al. (2024). Artificial intelligence-based classification of CT images using a hybrid SpinalZFNet. Interdisciplinary Sciences, 649. https://doi.org/10.1007/s12539-024-00649-4

[25] Aronson, L., Ngnitewe Massa'a, R., Jamal, S., Gardezi, S., & Wentland, A. L. (2024). Automatic segmentation of the kidneys and cystic renal lesions on non-contrast CT using a convolutional neural network. arXiv, 2405.08282. https://doi.org/arXiv:2405.08282

[26] Shorten, C., & Khoshgoftaar, T. M. (2019). A survey on image data augmentation for deep learning. Journal of Big Data, 6(1), 60.https://doi.org/10.1186/s40537-019-0197-0

[27] Krstinić, D., Braović, M., Šerić, L., & Božić-Štulić, D. (2020). Multi-label classifier performance evaluation with confusion matrix. Computer Science & Information Technology (CSIT), 10(8), 1–6. https://doi.org/10.5121/csit.2020.100801

[28] Mammola, S., Carmona, C. P., Guillerme, T., & Cardoso, P. (2021). Concepts and applications in functional diversity. Functional Ecology, 35(9), 13882. https://doi.org/10.1111/1365-2435.13882

[29] Liang, J. (2022). Confusion Matrix: Machine Learning. POGIL Activity Clearinghouse, 3(4). Retrieved from https://pac.pogil.org/index.php/pac/article/view/304

[30] Krstinić, D., Šerić, L., & Slapničar, I. (2023). Comments on 'MLCM: Multi-Label Confusion Matrix.' IEEE Access, 7672. https://doi.org/10.1109/ACCESS.2023.3267672